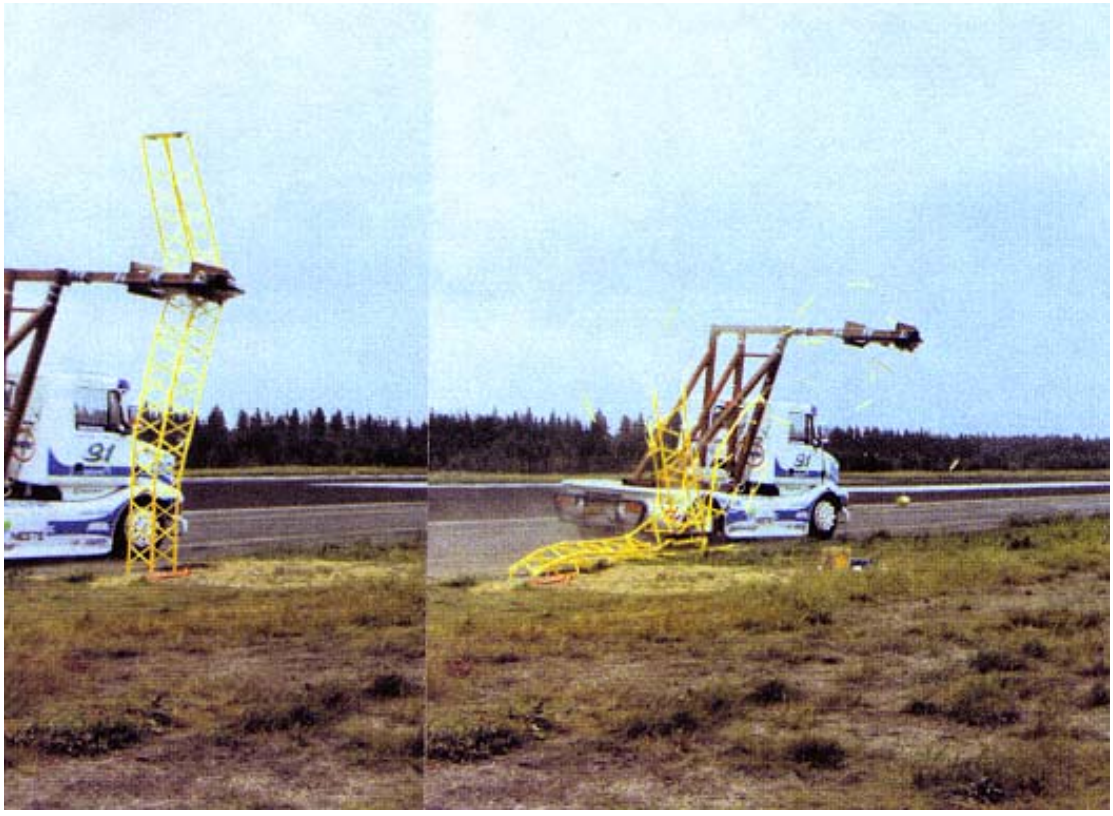

TEST REPORT
IMPACT TEST OF EXEL APPROACH LIGHT MASTS

Juhani Hanka
Markku Vahteri

OCTOBER 1991

Abstract

Horizontal impact tests on Exel airport approach light masts have been performed in order to evaluate the breaking, i.e. the frangibility, of the masts if impacted by an aircraft. A wing section attached to a high speed truck was used as an impactor. Impact energies were determined using the measured values of impact forces, the contact time and the speed. The damage caused to the wing section was carefully inspected to be able to estimate the effects of an impact on the performance of a real aircraft. The behaviour of the mast during the impact was investigated using the high speed camera documentation. Based upon these test results, the masts were considered to be frangible.

CONTENTS

CONTENTS 1
1 INTRODUCTION 2
2 OBJECTIVES 3
3 TEST SET UP 4
3.1 General description of the test procedure 4
3.2 Masts 5
3.3 Test equipment 6
3.3.1 Impactor 6
3.3.2 Force and acceleration measurement 7
3.3.3 Velocity measurement 8
3.3.4 Signal conditioning 9
3.4 Calibration of the test equipment 9
3.4.1 Load cells 9
3.4.2 Accelerometers 9
3.5 Photographic and video documentation 10
4. TEST RESULTS 12
4.1. Analysis of the recorded data 12
4.2 Investigation of natural frequencies 12
4.3 Final test results 13
4.3.1 Numerical results 13
4.3.2 Failure mechanisms 17
5. DISCUSSION 20
5.1 Numerical results 20
5.2 Failure mechanisms 22
6. CONCLUSIONS 23
7. SUMMARY 24
8. REFERENCES 25
APPENDIX 1 26
A1.1 Results from the test 1 26
A1.2 Results from the test 2 29
A1.3 Results from the test 3 32
A1.4 Results from the test 5 35
A1.5 Results from the test 6 38
A1.6 Results from the test 7 41

1 INTRODUCTION

At airports, approach lights are used to give approaching aircraft correct information of direction and distance to the runway. These lights are located at each end of the runways in a complex pattern consisting of a longitudinal main line several hundred meters long and of crossing lines of varying width. The level at which the lights are located is sloped down towards the end of the runway. These lights are set to their correct positions by the use of approach light masts.

Tight requirements have been set to the rigidity of the masts in the form of allowed angular deflections of the light beams. However, in case of a collision with a low flying aircraft, these masts should break with minimum damage to the aircraft, i.e. the masts should be frangible. The problem has typically been solved by applying one or several break-away points in rigid metal (aluminium) masts. This method -- although simple and practical -- has some disadvantages. E.g. the break-away point at the mast base is naturally rather insensitive to the cause of the load. The break-away loads may as well be due to natural loading, not an impact. The damage caused to an impacting structure is also greatly influenced by the overall mass of the mast. For this reason metal masts are not necessarily the ideal solution to frangible masts.

A completely different approach had been taken in the design of the composite Exel-masts of a lattice structure. They have been constructed by utilising the frangibility of the structure itself in case of a sudden impact. This built-in frangibility makes the separate break-away points unnecessary. When a non-impacting load or more evenly distributed load is applied (wind, jet blast), Exel-masts act as stiff and rigid lattice structures. The light weight of composites make them a suitable material for this application.

To assess the frangibility of a mast structure and to get absolute values of the impact energies, full scale impact tests are required. In this report the impact tests of Exel-masts have been described. These tests were performed on August 28th and 29th, 1991 at the Joensuu airport in Finland. The actual tests were performed by Neste Composite Technology, Neste Chemicals R&T, Material Research and Testing department and the local Exel Kivara Factory. Exel is a subsidiary of Neste and a part of Neste Composite Materials division.

2 OBJECTIVES

The first main objective of the tests was to evaluate the frangibility of Exel-masts. This required the determination of the impact forces, impact energies and contact times. A visual documentation of the mast behaviour during the impact and a close inspection of the damages suffered by the impactor were also considered most essential for the judgement of the frangibility.

Another main objective of the tests was to give guidance to the Frangibility Aid Study Group set by ICAO to develop new Frangibility Standards for Airport Approach Lighting. The aim of this group is to have the new standards finished and effective by 1993. It was considered especially important to present the frangibility of composite lattice masts to the group responsible for preparing the new regulations now, as the new standards will cover a much wider spectrum of airport masts than the present standards. The new standards will very likely be used for many years influencing the construction of airport lighting systems a long way into the next century.

3 TEST SET UP

3.1 General description of the test procedure

The tests were performed at the Joensuu airport, Finland. The tested Exel-masts were erected at one side of the airport runway. The masts were impacted by an aircraft wing section attached to a truck. At the impact, forces, accelerations and velocities were measured for later calculation of the impact energies. The tests were also recorded with several still cameras and a video camera for later evaluation.

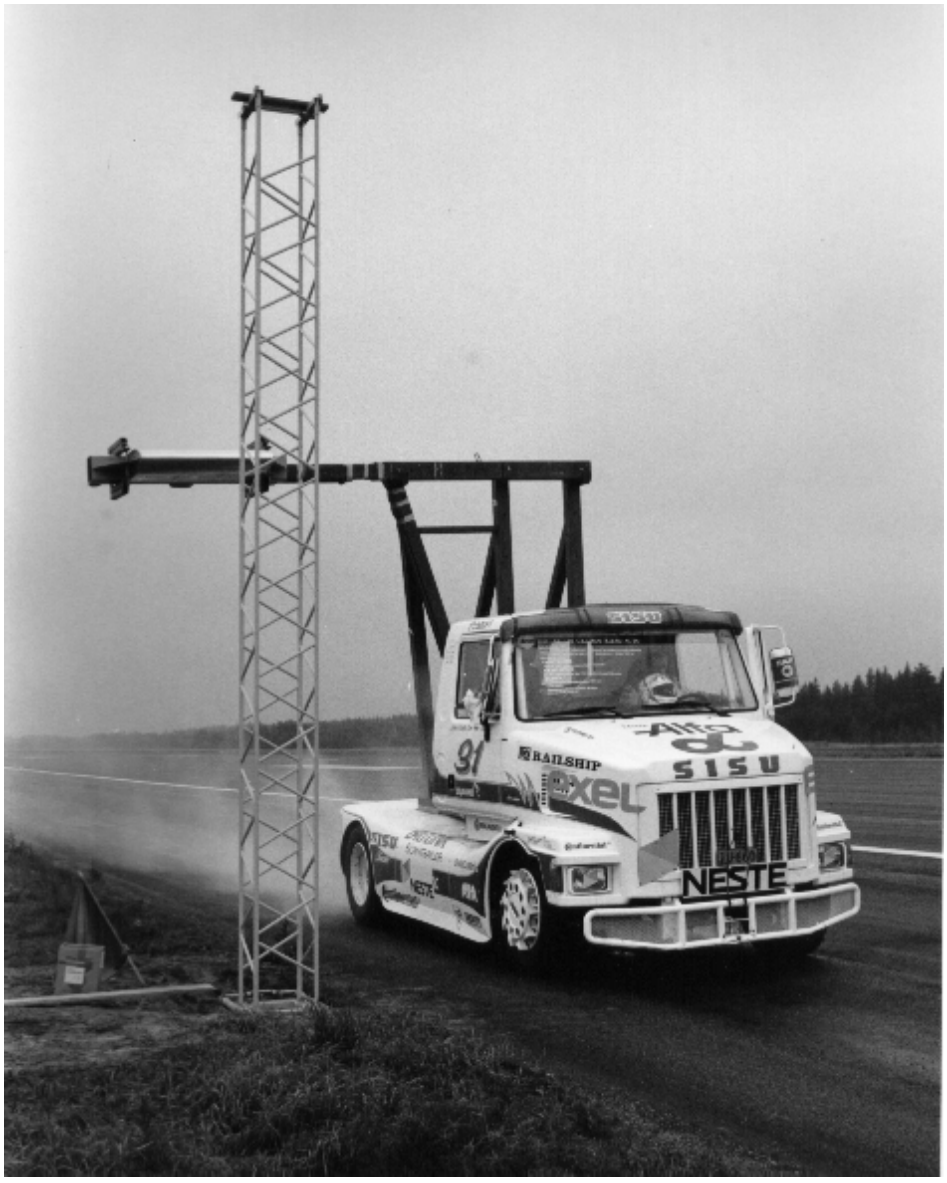

Figure 1 General view of the test set up.

The wing section was attached to the supporting cantilever beam via two load cells. From there the impact loads were transferred to the heavy supporting steel structure mounted on the bodywork of the truck. A 5-ton Sisu racing truck, competing in the European truck racing circuit, was used to give the impactor the required velocity.

3.2 Masts

Six individual tests were performed with identical mast configuration but with different arrangement with the lighting cables. All the masts were composite Exel-masts with following dimensions and features:

- composite lattice structure (glassfibre/polyester)
- square cross-section of 400 x 400 mm
- 6 meters in height
- top mass of 15 kg simulating the effect of a cross-bar with 3 approach lights
- vertical tubes ∅ 32/28 mm and diagonal tubes ∅ 22/18 mm

This mast configuration was selected since it was considered to be a representative example of typical approach light mast.

Three of the tested masts had no lighting cables since the frangibility of the Exel-mast structure itself was of primary interest. Because the cables have a great influence on the frangibility, three different arrangements for the cables were used in the remaining three tests. In the first one, the cables had two connection points at two meter intervals and the cables were located at the opposite side of the impact point. In the second and third mast there were no connection points along the mast. The second one had the cables on the side of the impact point and the third one on the opposite side. In all the three cases the cables were tightly connected at the top and at the base. The cables were inside of a protecting PVC-tube typically used for this purpose by the construction industry.

The masts were impacted at the height of 4.1 m.

Additional test was performed with a mast of completely different size and nature (test number 4, not reported here).

The test program is presented with the test results in chapter 4.

3.3 Test equipment

3.3.1 Impactor

In earlier tests /ref. 1/ a solid steel bar was used as an impactor. This allowed the measurement of the impact forces and energies. However, the extent of the damage to the aircraft structures could not be assessed. In addition, it was realised that the failure mechanism of the mast itself may have been affected by the type of the impactor. Due to the more brittle failure mechanism, the solid steel bar was considered to have been more favourable in regards to frangibility than a "softer" aircraft structure.

To eliminate the effects of a solid impactor and to be able to evaluate the behaviour of a real aircraft structure, a wing section was used as an impactor (fig. 2). The same type of wing section had been used earlier in tests of similar nature /2/. It is a structurally identical but aerodynamically simplified section of a Beech Queen Air type aircraft wing. This aircraft is a typical example of a lightweight (2 500 kg) commercial aircraft. 2 500 kg was earlier considered to be a suitable minimum mass under which a frangible mast should break. Recently this requirement has been set at the level of 3 000 kg /4/.

The wing section used was 1000 mm wide and 640 mm deep. The material used was 2024-T3 aluminium. It was backed by a steel column with a square cross-section of 200 x 200 x 6.3 mm. The wing section was riveted to the steel column acting as the main spar of the wing. To compensate the effects of the finite length of the wing section the outmost ribs were supported from outside. The idea was to prevent the unrealistic failure mode of the outer ribs collapsing inwards as observed in earlier tests /2/. The wing sections were manufactured by Valmet Aircraft Industries according to standard aircraft manufacturing procedures.

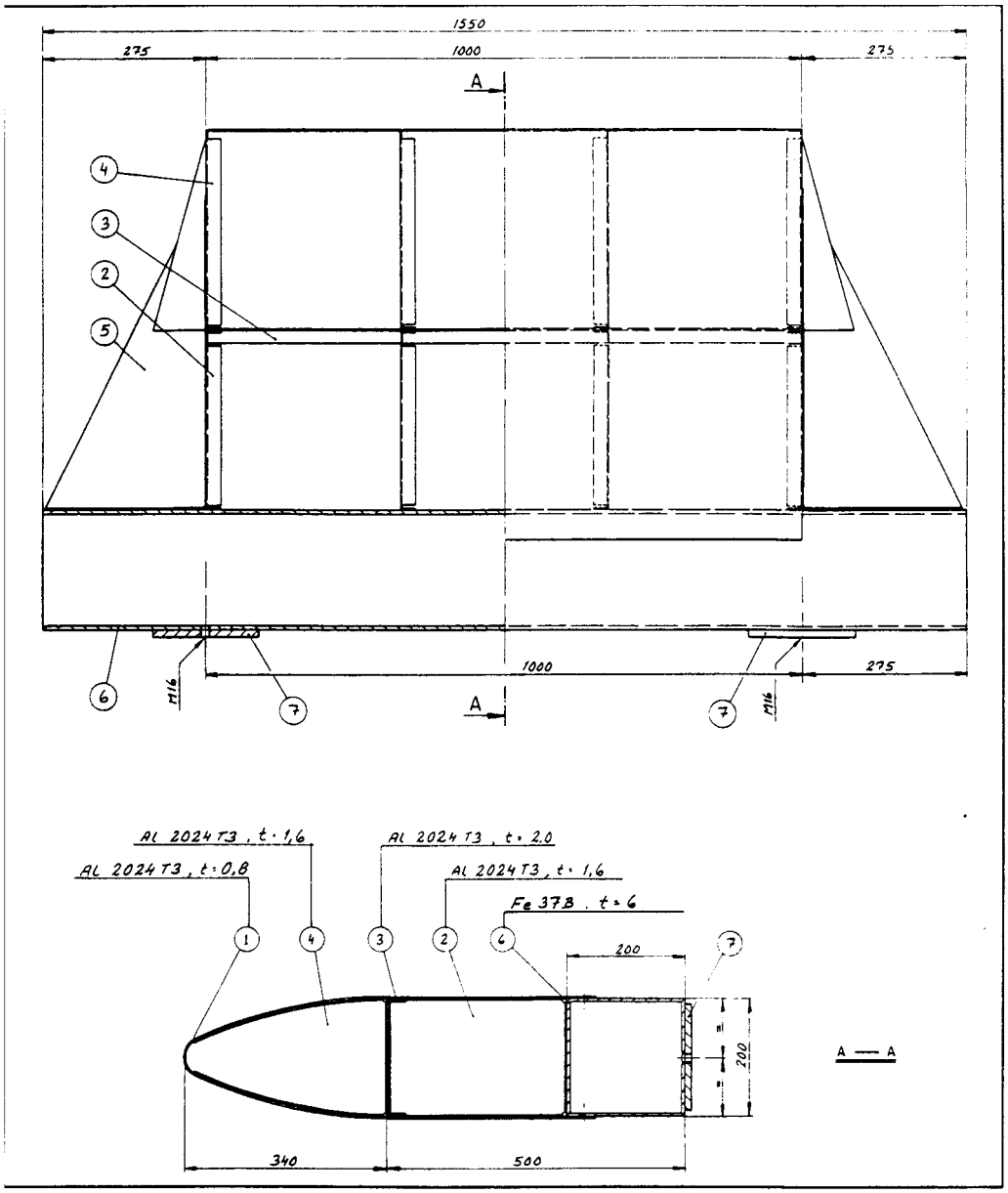

Figure 2 The structure and dimensions of the impactor.

3.3.2 Force and acceleration measurement

All the horizontal loads caused by the impact in the direction straight against the wing section were transferred through two load cells located between the wing backing column and the cantilever beam of the support structure. The load cells used were HBM Z7-2 ($\pm$20~kN) shear strain type load cells.

Two accelerometers were attached to the cantilever beam to measure both the horizontal and the vertical accelerations of the beam. Horizontally, the accelerometers were positioned in the middle of the wing section. The horizontal accelerometer used was a Bruel & Kjaer piezoelectric transducer of type 4391 (frequency response from 0.1 Hz to 12 kHz) and the vertical

accelerometer a Bruel & Kjaer piezoelectric transducer of type 4371 (frequency response from 0.1 Hz to 13 kHz). A schematic view of the measuring system is shown in Figure 3.

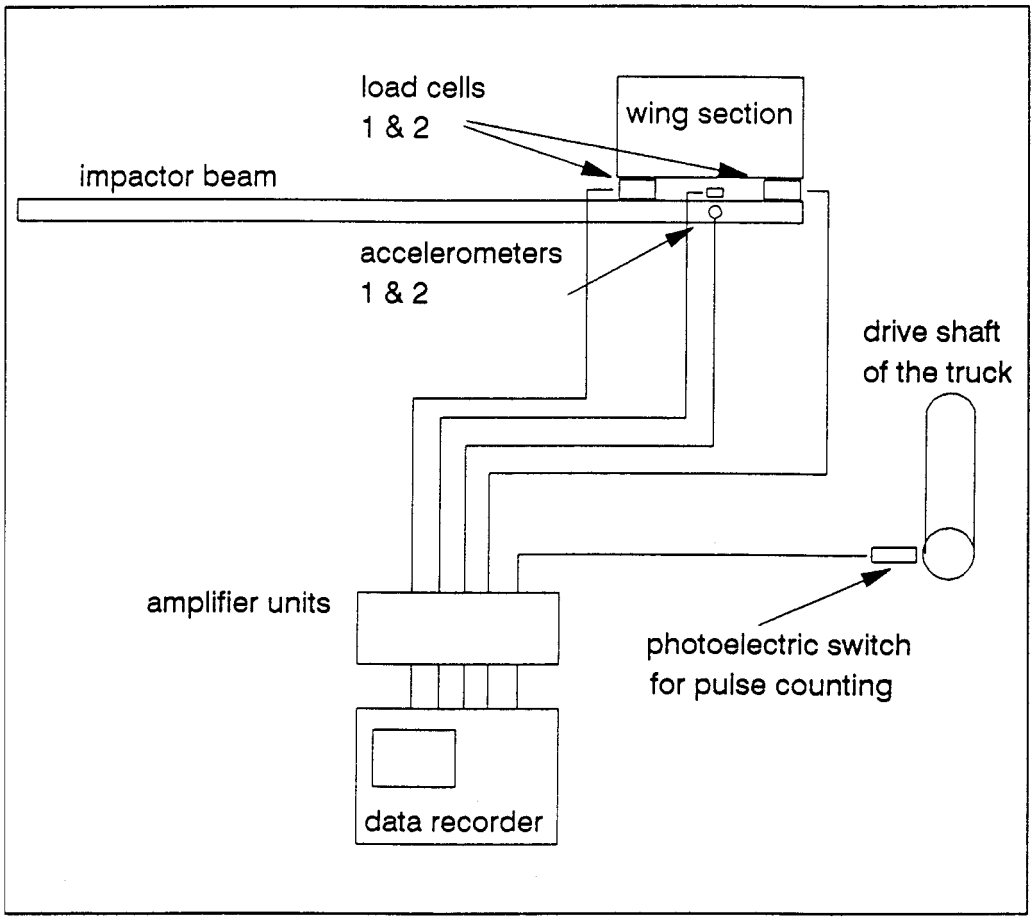

Figure 3 Schematic view of the measuring system.

3.3.3 Velocity measurement

A photoelectric pulse counter was used to monitor the revolutions of the truck drive shaft. The velocity calculation performed afterwards was based on the time difference between pulses. A radar was also used to confirm this velocity measurement and to get instant measurement after each test. As can be seen later from the final test results, these two velocities proved to be very close to each other.

The photoelectric switch used in the pulse counting was an Omron E3S-X3CE4 having an operating voltage from 12 to 24 V DC. A piece of reflecting tape on the drive shaft served as a pulse generator.

3.3.4 Signal conditioning

The force, acceleration and pulse signals were amplified and recorded by a data recorder for later analysis. All this equipment was located in the truck cabin.

The amplifiers used for load cells 1 and 2 were HBM K10C DCs (frequency response from DC to 10 kHz). The amplifier for accelerometer 1 (B & K 4391) was a Bruel & Kjaer charge amplifier of type 2635 (frequency response from 0.2 Hz to 10 kHz) and the amplifier for accelerometer 2 (B & K 4371) was a Kistler charge amplifier of type 5007 (frequency response from 1.6 Hz to 180 kHz).

A Teac XR - 50 H tape recorder with a tape speed of 38.10 cm/sec and a frequency response from DC to 10 kHz FM (frequency modulation) was used to record the measured data. For later analyses a digital oscilloscope of type Panasonic VP-5720A was used.

3.4 Calibration of the test equipment

3.4.1 Load cells

The calibration was carried out in the laboratory of Neste Chemicals R&T, Material Research and Testing department. Instead of the complete wing section only the steel backing column was attached to the load cells. The calibration load was introduced in the middle between the attachment points by an Instron servohydraulic actuator (Figure 4). The actuating force was measured using an Instron 50 kN load cell.

3.4.2 Accelerometers

Both of the accelerometers and amplifiers were calibrated using a calibrated vibration exciter Bruel & Kjaer Type 4294. The accuracy of the calibrator is better than ± 3 %.

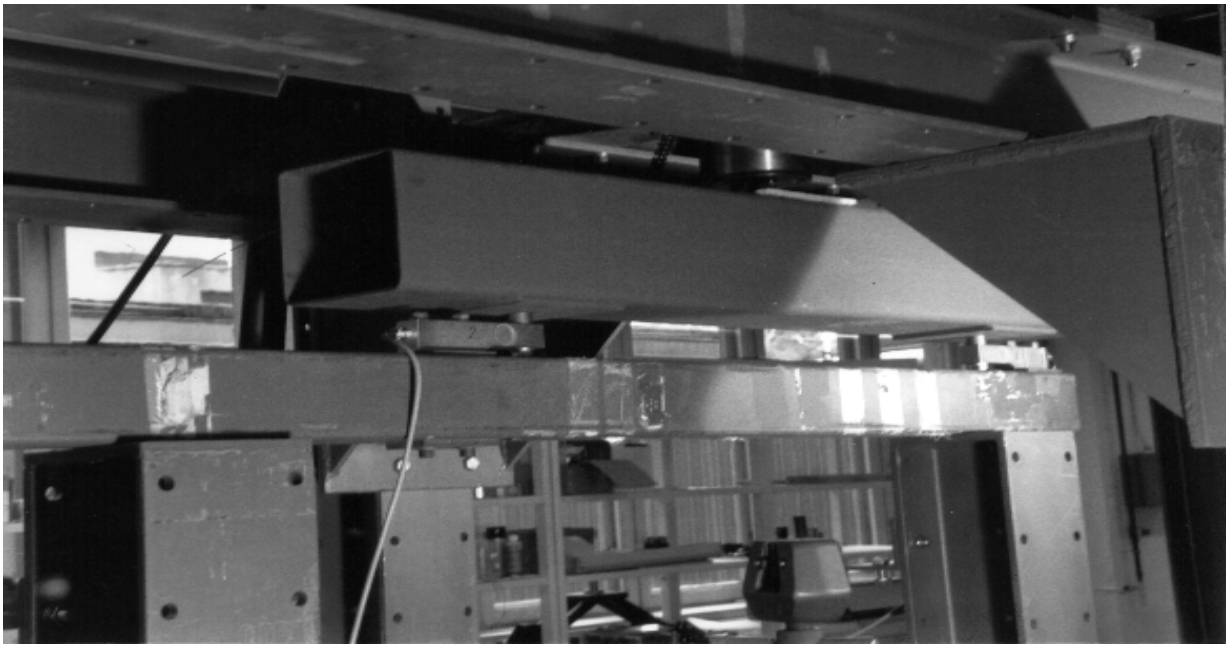

Figure 4 Calibration of the load cells.

3.5 Photographic and video documentation

A video camera was used to get a general view of the test procedure. A standard Sony M 3A colour video camera (25 frames/sec) was used.

A high speed film camera was used to record the behaviour of the wing section and especially the mast during the impact. The FASTAX 16 mm high speed camera used was capable of taking 2000 frames/sec. When developed, the film was converted into video mode. Finally this black and white video tape and the original colour video tape were edited to form a single visual document.

In addition, three automatic 35 mm cameras (Nikon F3, 5.5 frames/sec) were used to get the photographic documentation. One of the cameras was attached to the truck mirror handle to take single photographs at close range during the impact.

A schematic view of the photographic and video documentation set up is presented in Figure 5.

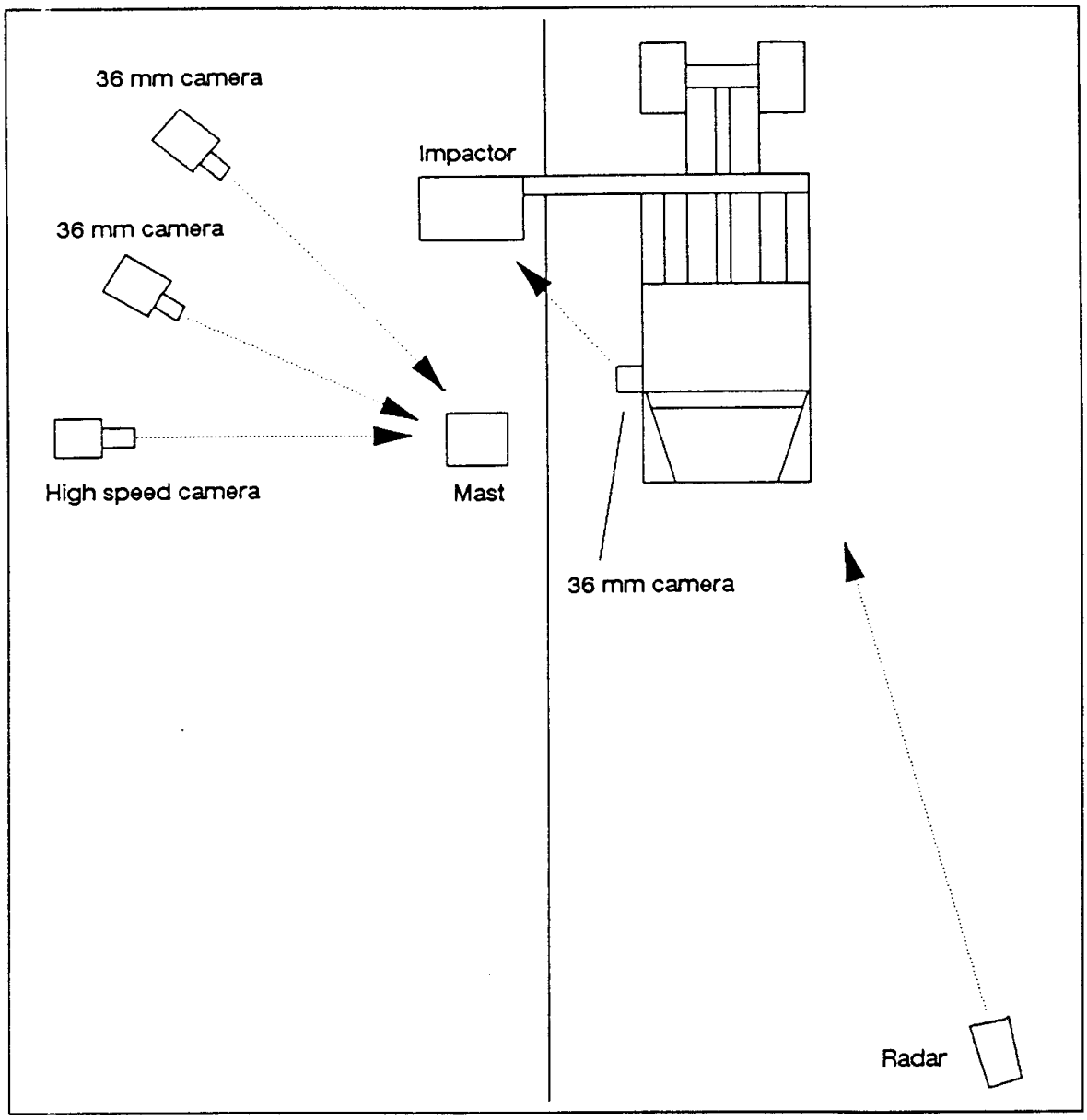

Figure 5 Schematic view of the photographic and video documentation set up.

4. TEST RESULTS

4.1. Analysis of the recorded data

The signals recorded at the field during the tests were then analysed to convert the information into a more usable form and to make all the necessary corrections. The recorded forces, accelerations and drive shaft pulse signals were fed from the data recorder to the digital oscilloscope. The force and acceleration signals were filtered with a 1 kHz low pass filter (90 dB/octave attenuation). The digitalized signals were transferred to a personal computer for further calculations.

The velocity of the impactor, i.e. the speed of the truck at the moment of the impact, was calculated by using the recorded pulse count vs. time data.

The absolute maximum value of the total force during the impact was determined to be the peak force. The total force was calculated as the sum of indications of the load cells 1 and 2.

The impact energy was determined by integrating the impact force with the forward movement of the impactor. The movement was reversly calculated from the recorded pulse count vs. time relationship (= time and velocity). The correction taking into account the proportional movement of the impactor and the truck body was calculated by using the horizontal acceleration measured by the accelerometer 1.

The contact time determination was based on the energy vs. time curve. The rise time from zero energy level to the maximum energy level was determined to be the contact time.

4.2 Investigation of natural frequencies

The natural frequency of the impactor assembly was determine by generating an impact with a rubber mallet. A relatively low natural frequency was found by analysing a "free run test", that is a test run at the speed of 140 km/h without external impacts. The interference caused by these natural frequencies were filtered from the recorded data in order to get the final results.

Two obvious horizontal natural frequencies were found: 184 Hz, local resonance frequency of the impactor and 6.3 Hz, which is a global resonance frequency of the whole system (the truck, the supporting structure and the impactor).

4.3 Final test results

4.3.1 Numerical results

The most important numerical test results were the velocity of the impactor, the peak force, the impact energy and the contact time of each test. These results are presented in the table 1. The forces and energies are also presented as curves. In this chapter, the curves for one test only are shown. Curves for all the other tests can be found in Appendix 1. Acceleration curves of test 1 are shown to give an idea of typical acceleration levels at the impact. Acceleration curves from the other tests have not been presented because of their marginal informative value.

The average value for the impact energy was 42.0 kNm. For the first three masts (no cables) the average impact energy was 36.7 kNm and for the last three masts (with cables) 47.3 kNm.

The test program is presented in the table 2. The program is needed to interpret the test numbers in table 1.

Table 1 The final test results.

Test number	Velocity (radar) km/h	Velocity (pulse count) km/h	Peak force kN	Impact energy kNm	Contact time ms
1	142	139.6	21.8	41.1	109
2	138	-*	29.5	35.8	107
3	144	144.8	26.4	33.1	96.1
5	140	139.6	33.3	44.9	165
6	142	142.8	31.0	54.7	151
7	142	142.6	23.8	42.4	113

* pulse counter failed

All the tests:
Average impact energy = 42.0 kNm
Standard deviation = 7.59 kNm (18.1 %)
Tests 1-3:
Average impact energy = 36.7 kNm
Standard deviation = 4.02 kNm (11.0 %)
Tests 5-7:
Average impact energy = 47.3 kNm
Standard deviation = 6.54 kNm (13.8 %)

Table 2 The test program. Note that in tests 5-7 the number of the connections only indicates the number of cable connection points along the mast. In all the cases, the cables were tightly connected at the top and at the base.

Test number	Cables	Connections	Cable location
1	No	-	-
2	No	-	-
3	No	-	-
5	Yes	2	Opposite side
6	Yes	No	Opposite side
7	Yes	No	Impact side

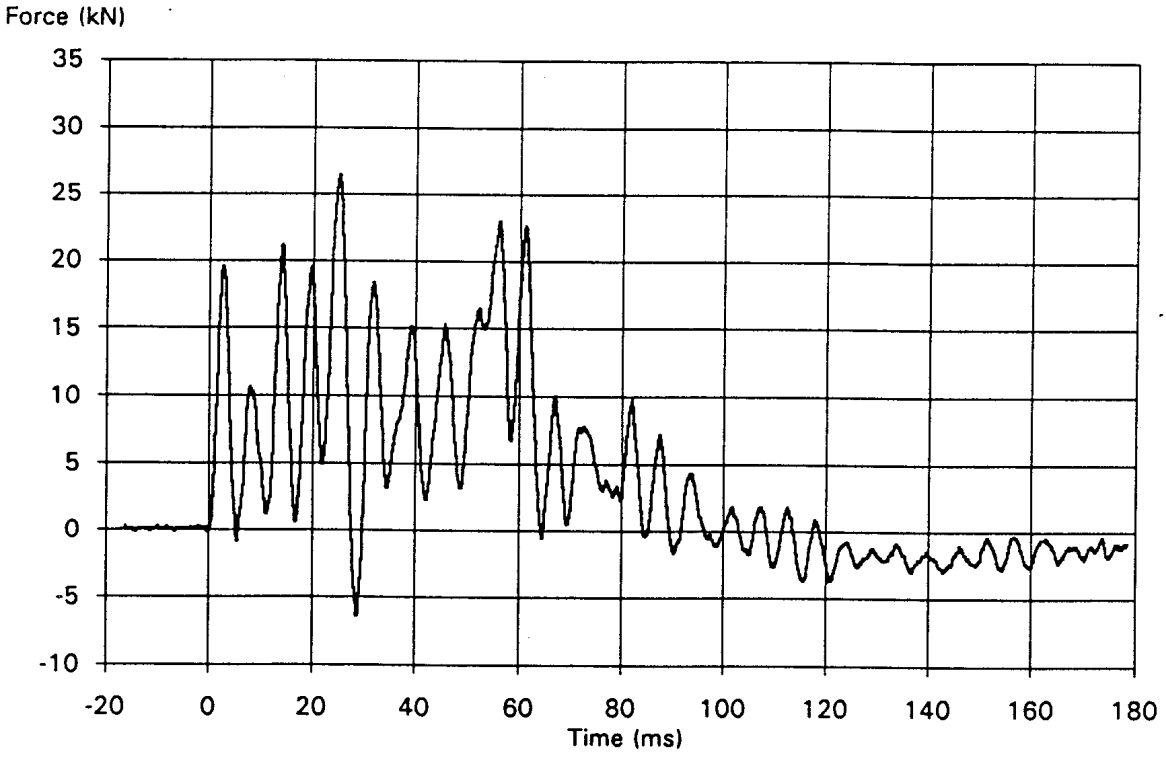

Figure 6 Example of a typical impact force vs. contact time curve (test 3).

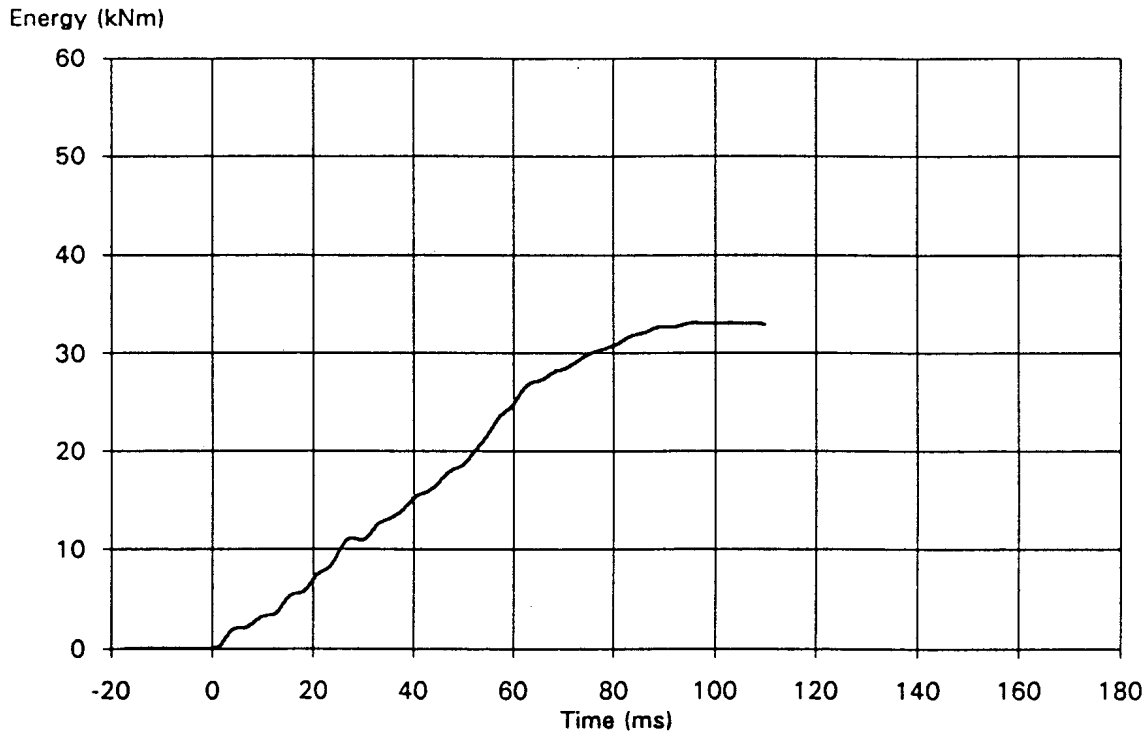

Figure 7 Example of a typical impact energy vs. contact time curve (test 3).

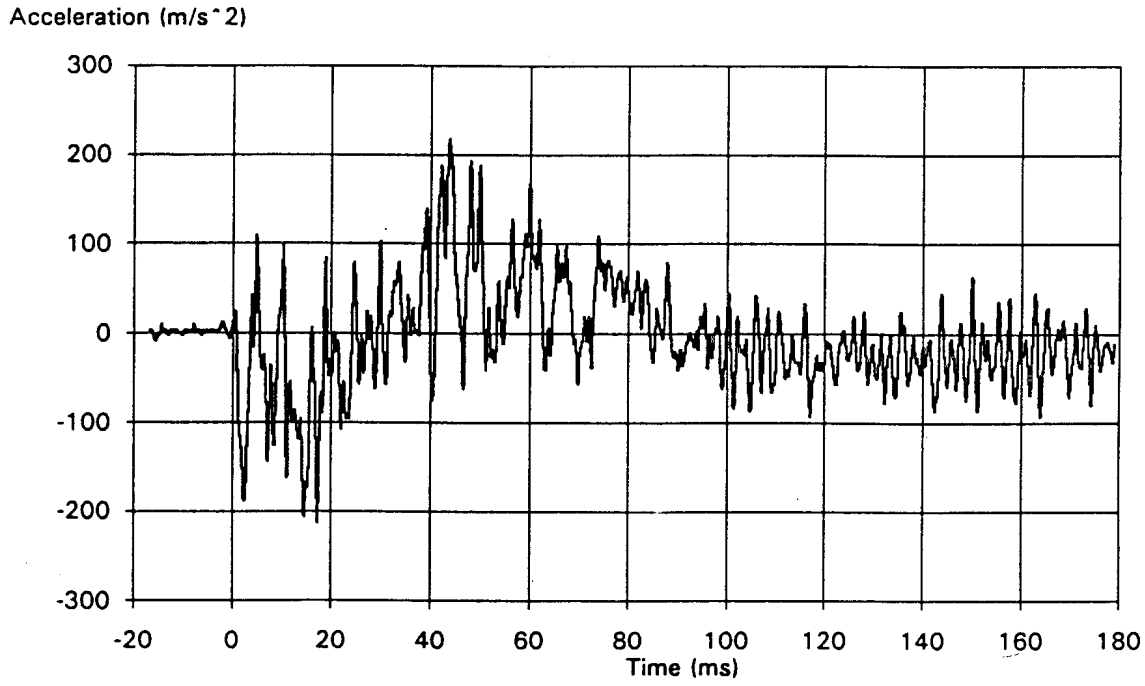

Figure 8 Example of a typical horizontal acceleration vs. contact time curve (test 1).

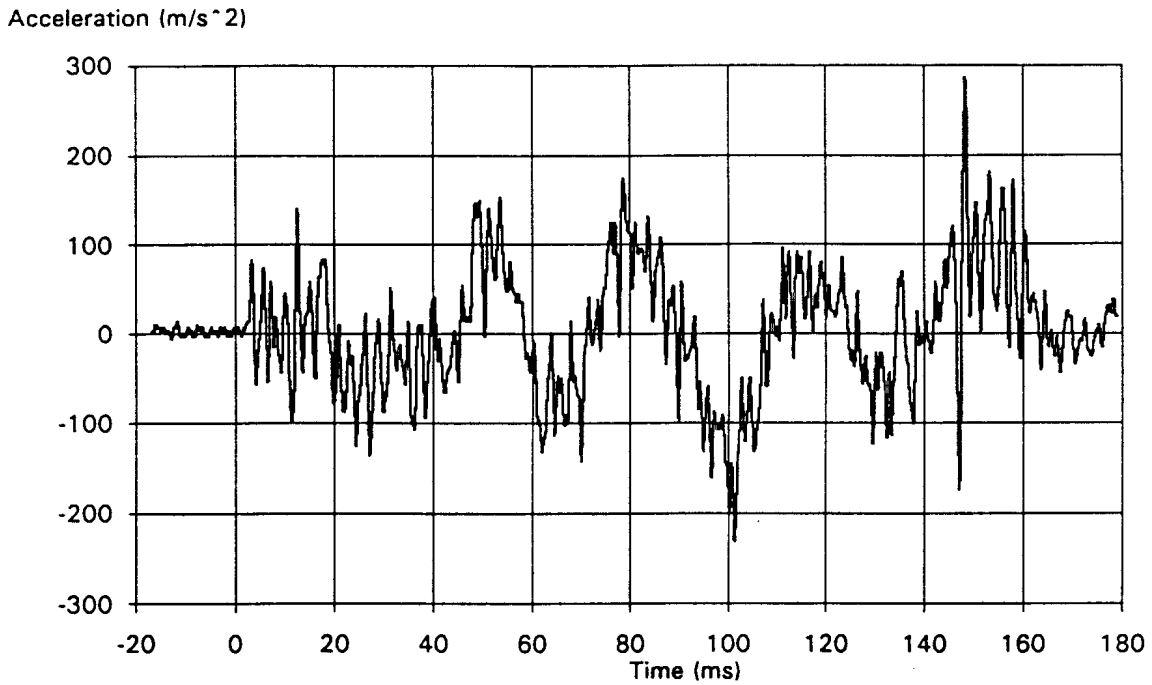

Figure 9 Example of a typical vertical acceleration vs. contact time curve (test 1).

In order to determine whether the significant differences in impact energies are partly due to the variations in velocities, the energy values were corrected by referring them to the velocity of 140 km/h. This was simply done by assuming that a certain kinetic energy (=velocity v) automatically leads to a certain impact energy W_i (subscript i refers to impact). This assumption can be expressed with the formula

$$W_{iref} = \left(\frac{v_{ref}}{v}\right)^2 W_i \qquad (1)$$

where $W_{i\,ref}$ is the "corrected" new impact energy. The results of this approach are presented in Table 3. From the results it can be noticed that the scatter is hardly reduced at all, thus proving that the effect of velocity variations is negligible when within certain limits. The differences in impact energies were probably caused by differences in the individual masts and by slightly varying conditions in each test. This also means that the discussion later on can be based upon the measured values, not on the corrected values.

Table 3 Impact energies referred to the reference velocity of 140 km/h. The original impact energies calculated from the measured data are shown for convenience.

Test number	Velocity (pulse count) km/h	Impact energy (measured) kNm	Impact energy (referred to 140 km/h) kNm
1	139.6	41.1	41.3
2	138*	35.8	36.9
3	144.8	33.1	30.9
5	139.6	44.9	45.2
6	142.8	54.7	52.3
7	142.6	42.4	40.9

* radar measurement

4.3.2 Failure mechanisms

In all the tests the masts broke in a frangible manner. Typically the masts broke into two main sections at about 1 - 3 meters above the ground level. The masts also broke into several smaller sections and into separate parts (= diagonals). This failure mechanism is clearly demonstrated in the pictures 10 and 11. The same behaviour is shown even better in the high speed camera recording (Appendix 2). Unfortunately there are only few informative photographs of the impact itself, because the standard camera used was rather slow (5.5 frames/sec) compared to the very short contact time (≈ 0.1 sec). In some tests (especially when the cables were used) part of the damaged mast showed a tendency to wrap around the wing section or to get stuck with the torn aluminium skin. The part that wrapped around (or bent around) the wing was the "rear" plane of the lattice structure, i.e. the two vertical tubes and the connecting diagonals at the opposite side of the impact . The 15 kg weight at the top of the mast always fell within 2 or 3 meters from the base plate. In the wing sections the damages where limited to the leading edge area. The very thin 0.8 mm skin was severely damaged between those ribs where the mast was hit. Due to the dimensions of the wing and the mast, the mast was typically impacted so that two out of the three rib sections (= a section between two ribs) were hit by the mast and the third rib section remained undamaged or showed substantially less damage.

In all the wing sections the penetration of the mast into the wing structure was stopped before the front spar or by the front spar (the front spar is the first spanwise "beam" in the wing structure, see Figure 2). The front spar always remained intact. The wing skin was not damaged further back from the front spar. Local buckling of the skin panels occurred in some cases right behind the spar. The rivets used for riveting the skin to the ribs in the damaged areas were mainly cut by shear. Only few of the skin/front spar rivets failed.

In this chapter only typical pictures of the impact and of the damaged wing section are shown. A full photographic documentation of all the tests can be found in Appendix 1 with a complete set of the numerical results.

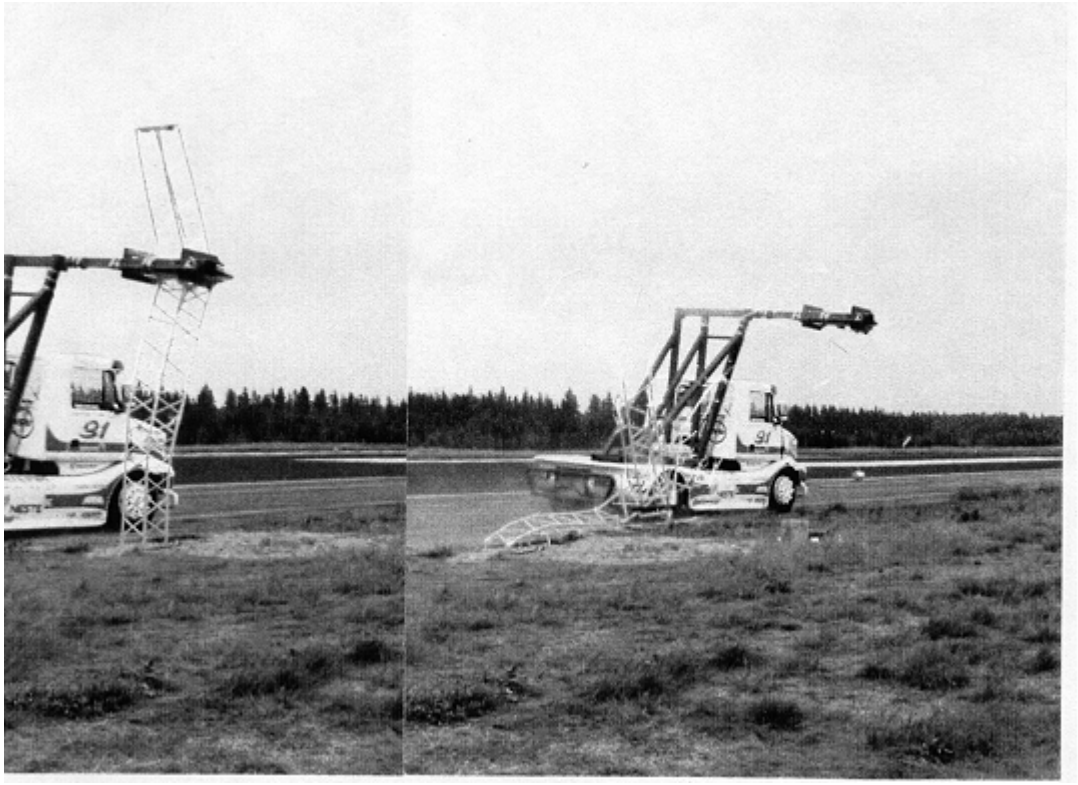

Figure 10 Mast 3 during the impact.

Figure 11 Remains of the mast 2 after the test.

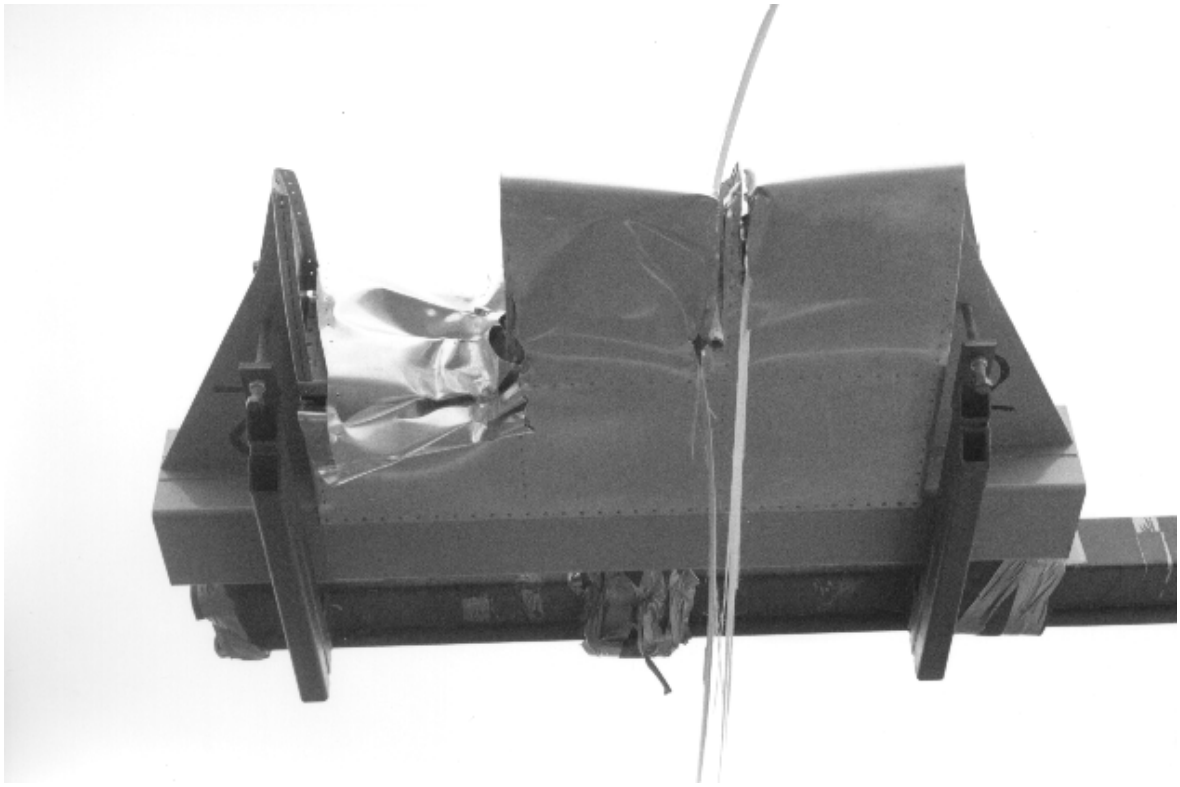

Figure 12 Damaged wing section after the test 2. The leading edge skin panels were severely damaged but the inner load carrying structure remained intact.

5. DISCUSSION

The final test results have to be analysed using two different methods. At first by analysing the numerical values, mainly the impact energies, and then by inspecting thoroughly the photographic and video documentation to determine the failure mechanisms and the extent of failure.

5.1 Numerical results

The most important interpretation of the numerical data is what the consequences would be to a real aircraft. One of the risks is that even if the aircraft survived the collision without loosing its structural integrity, it would loose so much of its kinetic energy (= velocity) that it would stall or otherwise loose the manoeuvrability. The loss of velocity can be theoretically derived from the fact that kinetic energy after the impact is the original kinetic energy minus the impact energy. This leads to a simple formula where the change in velocity Δv, i.e. the velocity loss, can be expressed as

$$\Delta v = v0 - \sqrt{v_0^2 - 2W_i/m} \qquad (2)$$

where v_0 is the velocity of the impactor before the impact, W_i the measured impact energy and m the mass of an imaginary aircraft.

In table 4, velocity and energy losses for two different aircraft weight categories are presented. In the first case (a 3 000 kg aircraft) referring to the ICAO-requirements, the velocity loss is between 1 and 2 km/h, which can hardly be considered critical. The other case, 80 000 kg, was calculated only to demonstrate the negligible effect of frangible masts of this type for a medium-class passenger transport aircraft (MD-80 series or an equivalent).

Table 4 The loss of total kinetic energy and velocity due to the impact for two different aircraft weight categories.

Test number	Impact energy	Energy loss		Velocity loss	
	kNm	3 000 kg %	80 000 kg %	3 000 kg km/h	80 000 kg km/h
1	41.1	1.82	0.07	1.28	0.048
2	35.8	1.62	0.06	1.13	0.048
3	33.1	1.36	0.05	1.00	0.037
5	44.9	1.99	0.07	1.40	0.052
6	54.7	2.32	0.09	1.66	0.062
7	42.4	1.80	0.07	1.29	0.048

The results seem to be in fair accordance with earlier results. If the impact energies measured with the solid impactor /1/ are referred to the velocity level of 140~km/h using eq.\ (1), they give an average value of 46.6~kNm. The difference to the present case is explained by heavier mass on top of the mast (30~kg in ref.\ /1/). This accordance is encouraging since it shows that the test procedure used is adequately repeatable despite the reasonably high scatter. This is a sign of reliability that also makes these results increasingly useful for the frangibility evaluation in general. Based upon these results, it is obvious that three tests per mast configuration should be a minimum requirement. It would be very difficult or misleading to draw conclusion from a smaller amount of tests.

The results presented in the table 1 also clearly indicate that the impact energies of the masts with cables were substantially higher than the energies measured for masts only. The average values show an almost 30\% increase in energy due to cables. This is very likely an exaggerated figure since it results partly from the very high single measured values of test 5. However, this difference is a sign of a definite trend. Not counting the lowest and highest measurements reduces the difference only to a 15 -- 20\% level. It can not be said, whether this difference is due to the cables only. The cover tube may also have an effect of some significance.

Although the tests proved to give reliable results and a great deal of valuable information, one major problem still exists. It is not known how these test results apply to different mast configurations. There should be established procedures, commonly approved for, how to derive the frangibility properties from one test series for a whole family of similar structures. The applicability range of one test series should also be determined. It is strongly recommended that rules or guidelines for this kind of a frangibility evaluation should be included in the new standard regulations. Naturally, these rules would apply only inside a certain family of structures which are known to have the same failure mechanism. It has to be pointed out that although rules are required, it is obvious that too tight limits, e.g.\ for the applicability range of tests, would result in a devaluation of

the regulations. The amount of tests required (and the regulations in general) has to be in balance with the resources and capabilities of the manufacturers. Complete testing of several different mast sizes and configurations would not be a realistic requirement, since full scale impact tests are extremely expensive. Because no regulations of this kind exist so far, it is assumed that the results of these tests can be considered to apply to all Exel airport masts of similar structure.

5.2 Failure mechanisms

The most important result from these tests in general was the fact that the tested masts did not break the wing structure. At the first sight the damages suffered by the wing section appeared to be quite severe. Closer inspection soon revealed, however, that the wing load carrying structure -- the frame work of spars and ribs -- was not damaged at all. The aerodynamic shape of a narrow leading edge section was lost with the crushed leading edge panels. The torsional stiffness was also slightly reduced since this nose section forms a part of the wing torsion box. The effect of this reduction is minimal. What is more important, the capability of the structure to carry bending and shear loads was not affected at all.

The failure mechanism of the masts could be described as frangible. Typically the masts broke away, leaving no or only minor parts of the mast attached to the damaged wing. The maximum weight of the parts left hanging from the wing, was between 4~--~5~kg (about 1.4~kg/m). These structurally damaged, partly disintegrated remains of the mast can hardly be considered as a risk. If the parts hanging from the wing tended to get stuck to another mast in the line, it would most likely lead to a complete disintegration of those parts, with minimum further damage e and velocity loss to the aircraft.

It can be concluded that the wrapping tendency that occurred especially with the masts with cables, was not critical but should be removed. Partly the wrapping was caused by the cables (and the cover tube) which did not always break as wanted. This can be avoided with additional connection points in the cable.

Another reason to the wrap-around was the composite structure itself. This was detected especially in test 1. Longitudinal splitting of the composite structure in the vertical tubes prevented the cut-through of the tubes at the opposite side of the impact. It has been assumed that a small change in the tube structure would turn the crack growth in the tube wall partly in transverse direction, thus helping the vertical tubes to cut apart more easily, in case of a sudden impact.

6. CONCLUSIONS

These impact tests of Exel approach light masts clearly showed that impact energies experienced at the collision of an aircraft wing with an Exel-mast are relatively small in relation to the kinetic energy and velocity of the aircraft. Even in the most critical weight class (3 000kg), the theoretical velocity loss was found to be less than 2~km/h (provided that the velocity is about 140~km/h). For heavier aircraft the velocity loss would be negligible. A velocity loss of this magnitude is far from critical and cannot stall an aircraft, not even in take off or landing.

Somewhat higher impact energies were measured for the masts with cables, although the energy level was still reasonably low. The cables also seemed to increase the tendency of the mast to wrap around the wing. This indicates that better failure mechanisms for the cables and more suitable cover tubes should be developed or alternative approaches should be taken. For the time being, the problem can be dealt with adequately by using break-away points in the cables and cover tubes, but a more favourable solution should be sought after. The possibility to further improve the failure mechanism of the mast itself by changing the tube structure has to be thoroughly investigated.

The damages caused to the wing sections by the impact were mainly superficial. The leading edge section covered only with 0.8 mm aluminium skin was damaged in the narrow section, where the mast was hit. The front spar and the load carrying structure further back were not damaged at all. It can be concluded that the capability of the wing to carry aerodynamic loads was not reduced. From a structural point of view, it is evident that an aircraft, even in the most critical category, damaged by a collision with the tested masts during the approach, would be able to continue flying and make a safe landing. In the scope of these results, it also seems that in case of a collision at the take off, the aircraft would be able to get more height, turn back and land safely.

The video tape based on the high speed camera film and the photographs, are an extremely important aid in evaluation of the frangibility of the Exel-masts. With the experience of all the tests performed with Exel-masts, it can be said that no decisions concerning the frangibility of a single mast type or frangibility in general should be based upon numerical data only. The photographs and the video tape of these tests may prove to be useful also for the Frangibility Study Group.

From these results and from the recorded failure mechanisms of the masts itself, it can be concluded that the tested Exel-masts are frangible structures that could remarkably increase aviation safety.

7. SUMMARY

The frangibility is the most important requirement concerning the masts used for airport approach lighting in addition to the structural requirements. The masts are required to have special break-away points or built in frangibility, so that if impacted by an aircraft, the mast would fail without serious damage to the aircraft.

In these tests the frangibility of Exel airport approach light masts was evaluated. The masts were of composite lattice structure. The tests were performed by impacting Exel-masts of a typical configuration with an aircraft wing section. Six masts were tested. During the impact, critical parameters like impact energy, impact force, contact time and impactor velocity were measured. The tests were also documented using a high speed camera, several standard cameras and a video camera for later evaluation.

The tests showed that the impact damaged only the leading edge skin panels of the wing section. The load carrying wing structure was not damaged. The determined impact energies proved to be reasonably low in relation to the kinetic energy and velocity even for the most critical minimum weight category aircraft. This results in a very small velocity loss suffered by the aircraft at the impact. The failure mechanism of the mast was found to be of frangible nature although some tendencies for the mast to wrap around the wing was detected. This behaviour was not considered to be critical, because of the marginal mass and the disintegrated nature of the parts wrapped around the wing. Recommendations were made for changes in the mast structure to prevent this behaviour.

It was concluded that in these tests Exel-masts proved to be frangible in case of a sudden impact. It was also understood that the results from these tests in general would be useful to the Frangibility Aid Study Group working for ICAO to set up new frangibility regulations for all airport masts.

8. REFERENCES

/1/ Eero Sallinen and Markku Vahteri: Horizontal Impact Tests on Approach Light Masts. Test Report, Neste Corporate R&D, Materials Research Department. Finland 1990.

/2/ J. Olthoff: Impact Testing of a Full Scale Frangible Approach Lighting Structure. NLR Contract Report, National Aerospace Laboratory NLR, The Netherlands.

/3/ Göran Eriksson: Horizontal Impact Tests on Approach Light Masts. Test Report, Swedish Board of Civil Aviation, Technical Department. Sweden, 1985.

/4/ C. Devasenapathy: New Specifications for Navigational Aids Will Include Built-in "Break-away" or Failure Mechanism. ICAO Journal, June 1991.

APPENDIX 1

A1.1 Results from the test 1

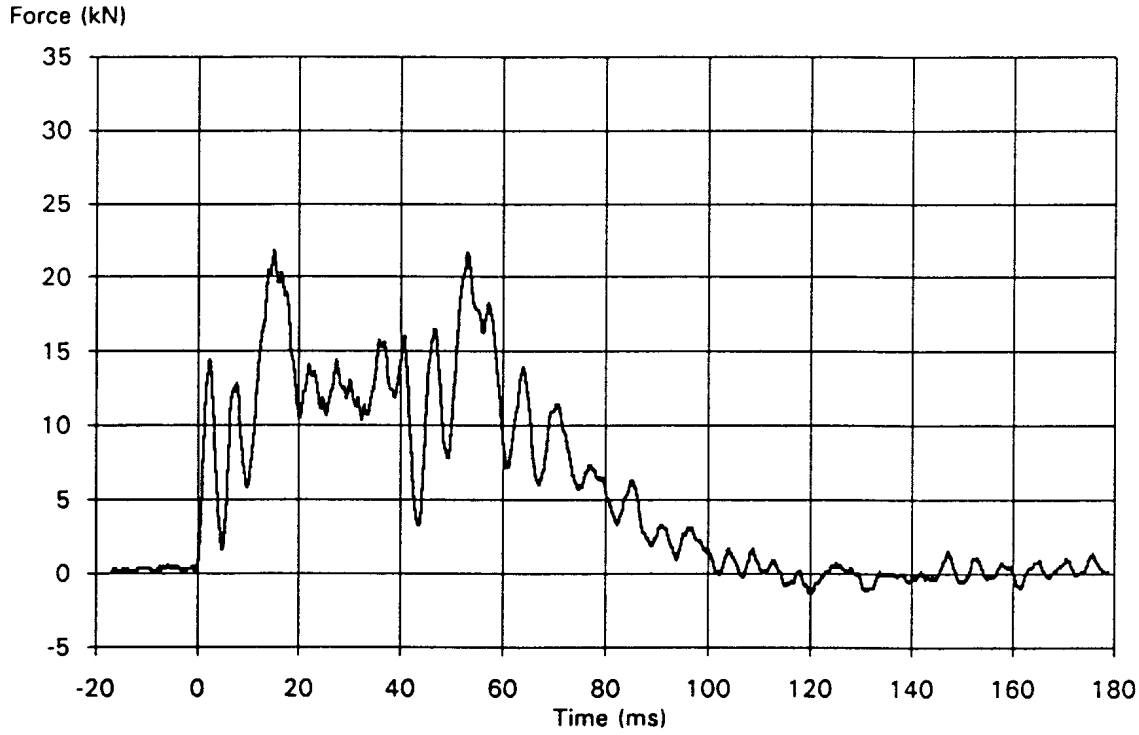

Figure A1.1 Impact forces vs. contact time.

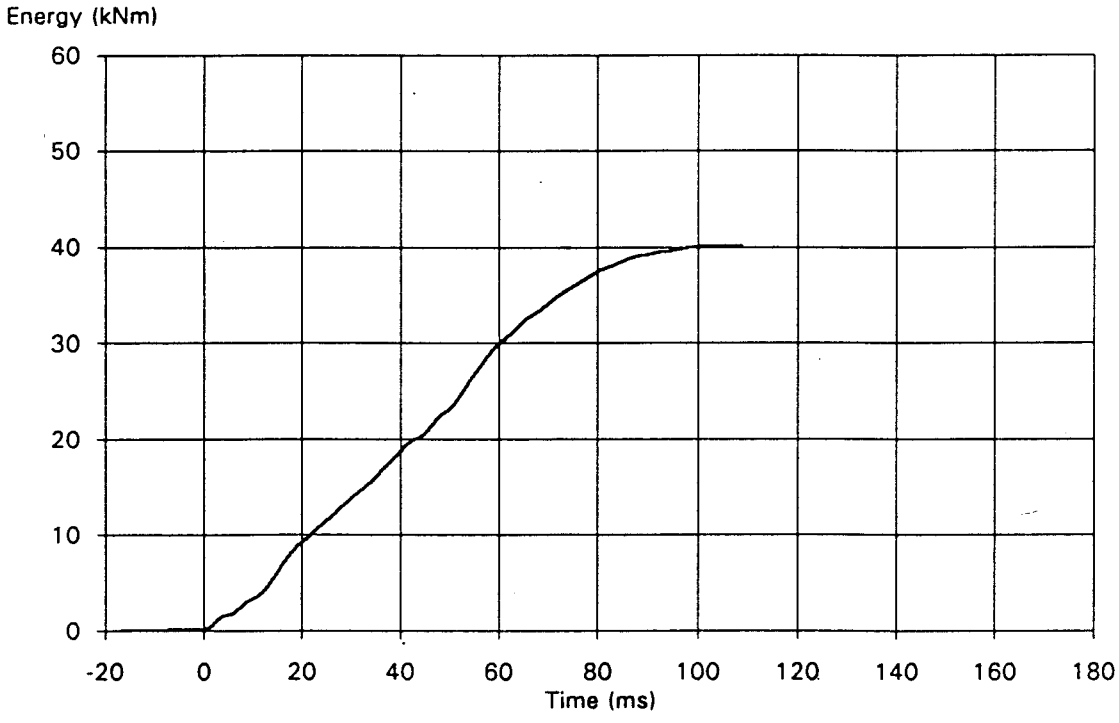

Figure A1.2 Impact energy vs. contact time

Figure A1.3 Test wing section immediately after the impact. Part of one side of the mast remained hanging from the wing. In this case it was completely loose, it did not get stuck. Note that the penetration has stopped at the front spar and that in the outmost rib section even the thin skin panels remain undamaged.

Figure A1.4 The lower section of the collapsed mast. The mast was cut n the middle at the impact side and almost at the base at the other side. It also broke into two parts longitudinally which can be seen also from the previous picture. Note the fallen weight in the upper left corner.

Figure A1.5 The damages caused to the wing are clearly visible in this picture. The 0.8 mm skin has been torn and crushed, but the front spar has not been touched. The only damages further back are the small buckle in the rightmost panel and three loose rivets (rib/skin joint in the middle).

A1.2 Results from the test 2

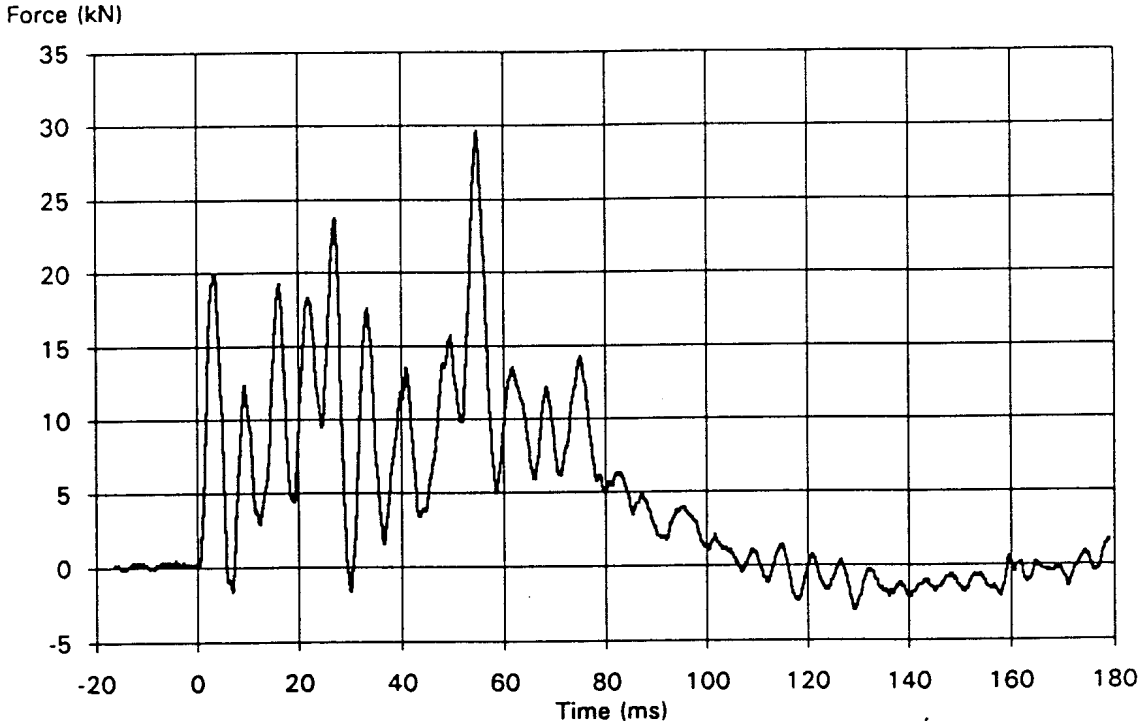

Figure A1.6 Impact forces vs. contact time.

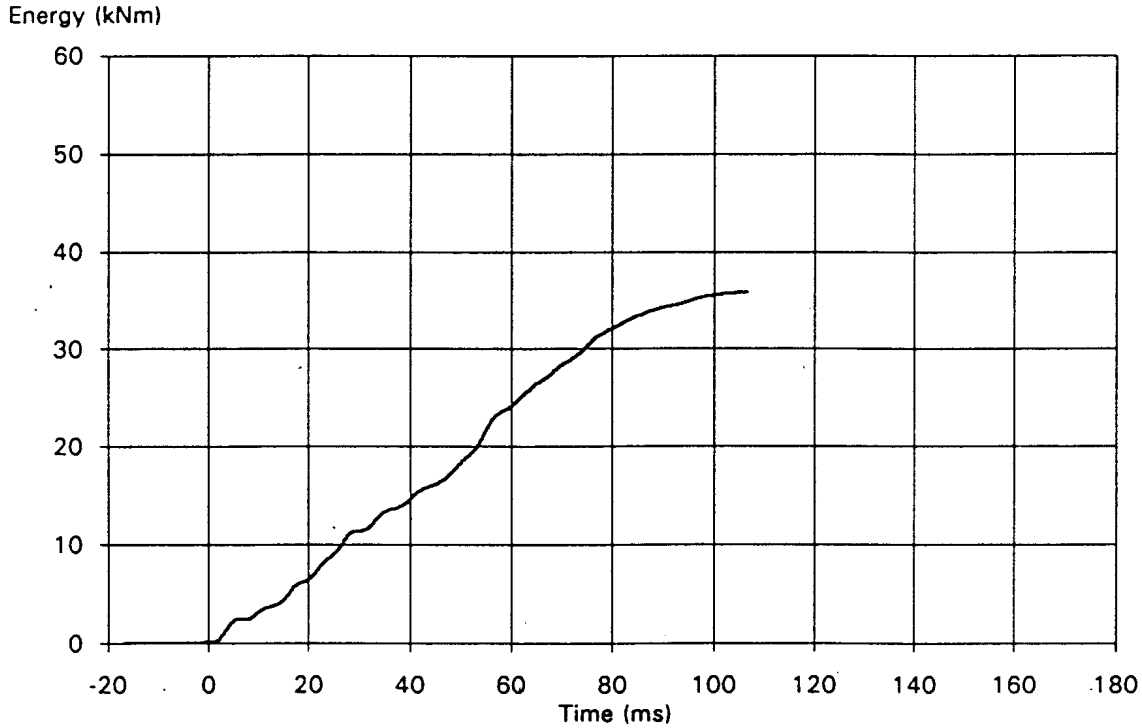

Figure A1.7 Impact energy vs. contact time.

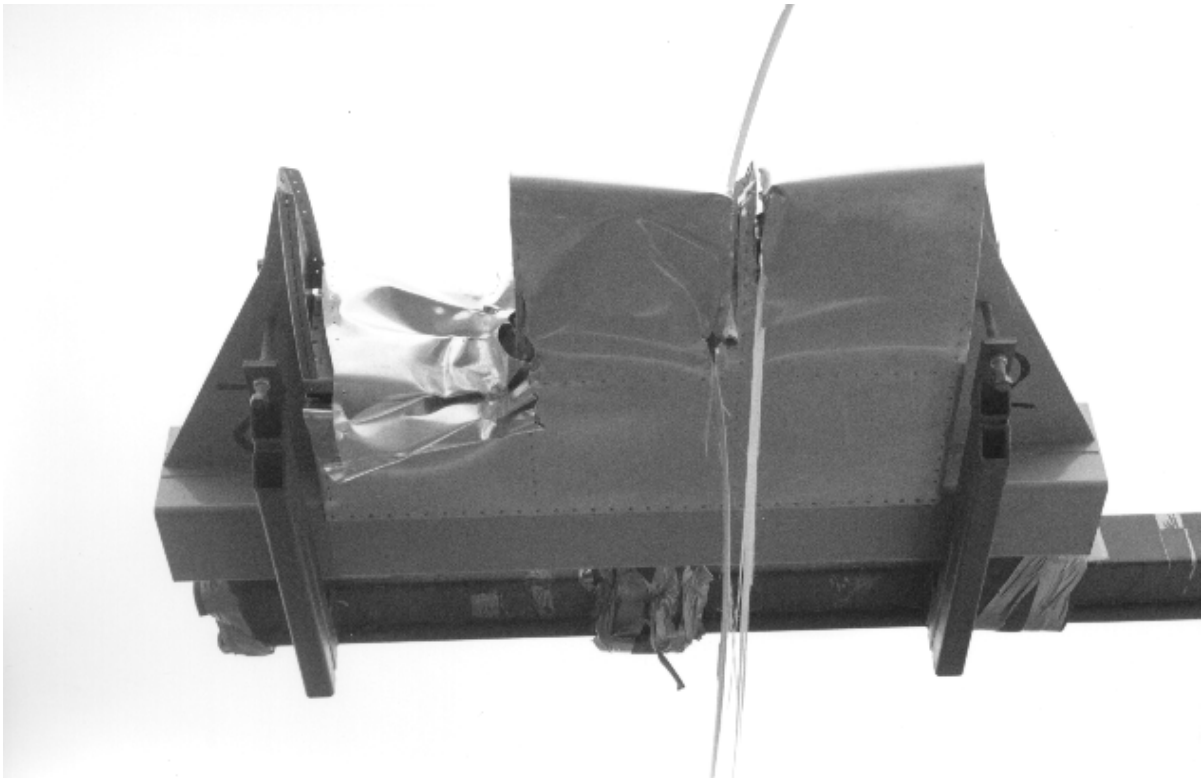

Figure A1.9 The outmost rib section was crushed as in test 1, but a few rivets from the skin/front spar joint were cut. Also the other two rib sections were torn apart from the ribs by long split fibres of the "rear" (=opposite side to the impact) vertical mast tubes. This was the only test when this occurred.

Figure A1.10 The mast broke into two main sections and into numerous separate parts.

Figure A1.11 The unique failure mode of this test is clearly visible. The front spar was not damaged despite the cut rivets.

A1.3 Results from the test 3

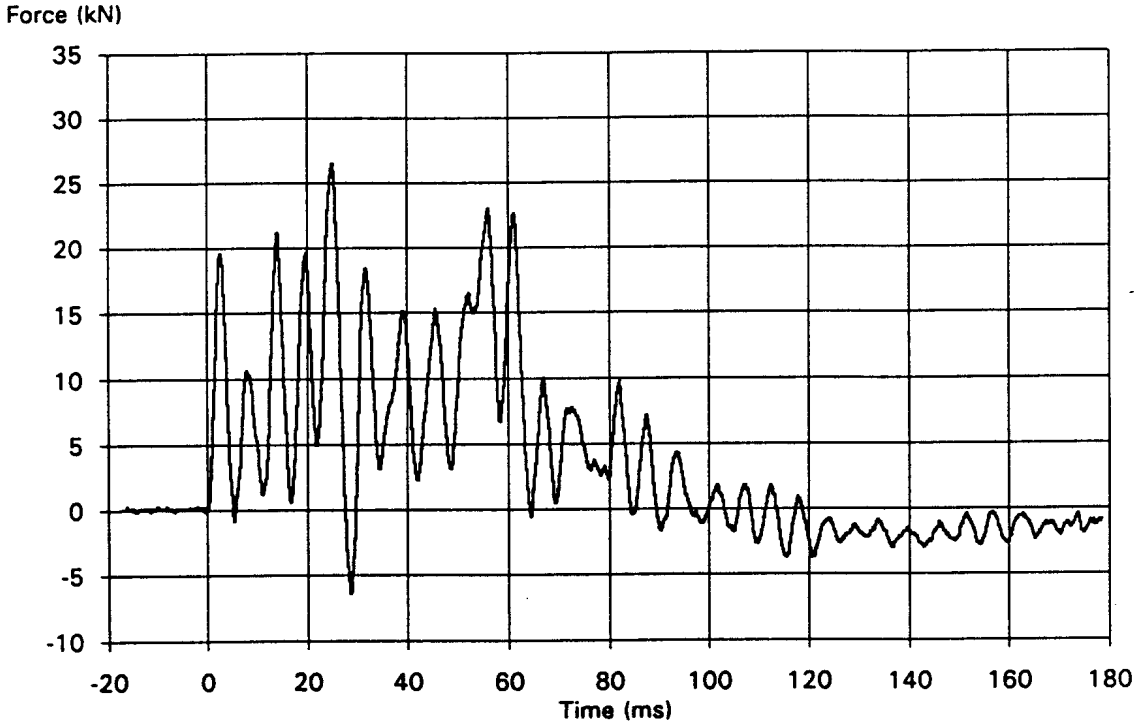

Figure A1.12 Impact forces vs. contact time.

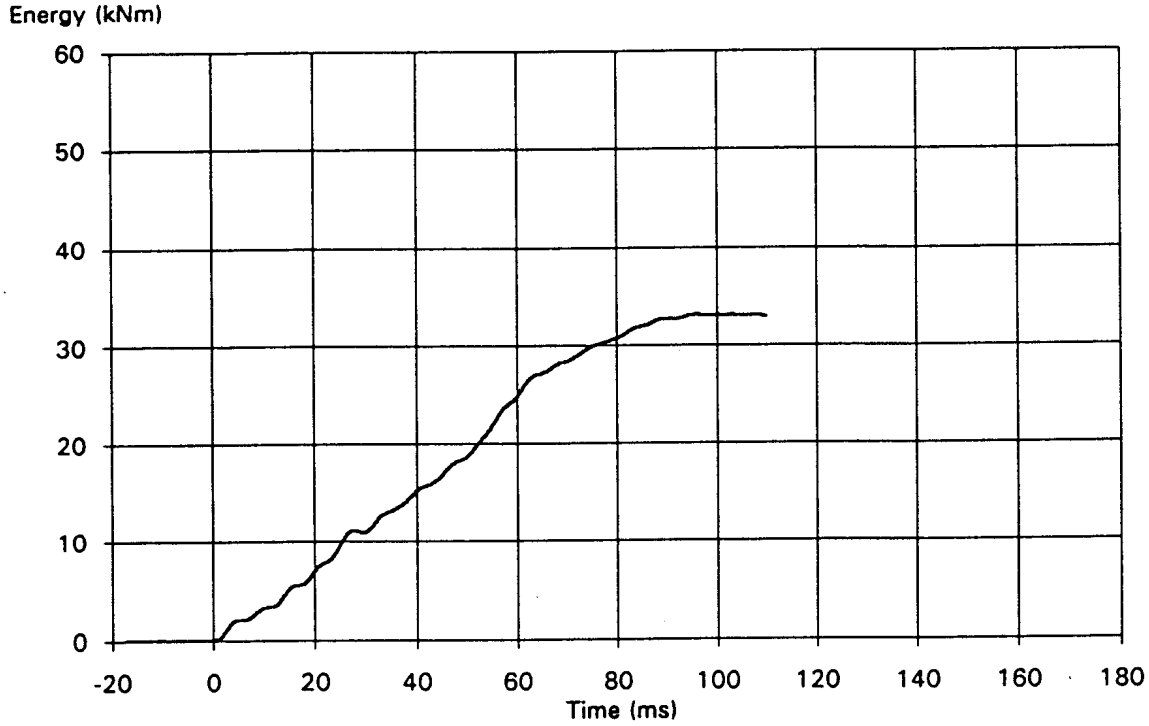

Figure A1.12 Impact energy vs. contact time.

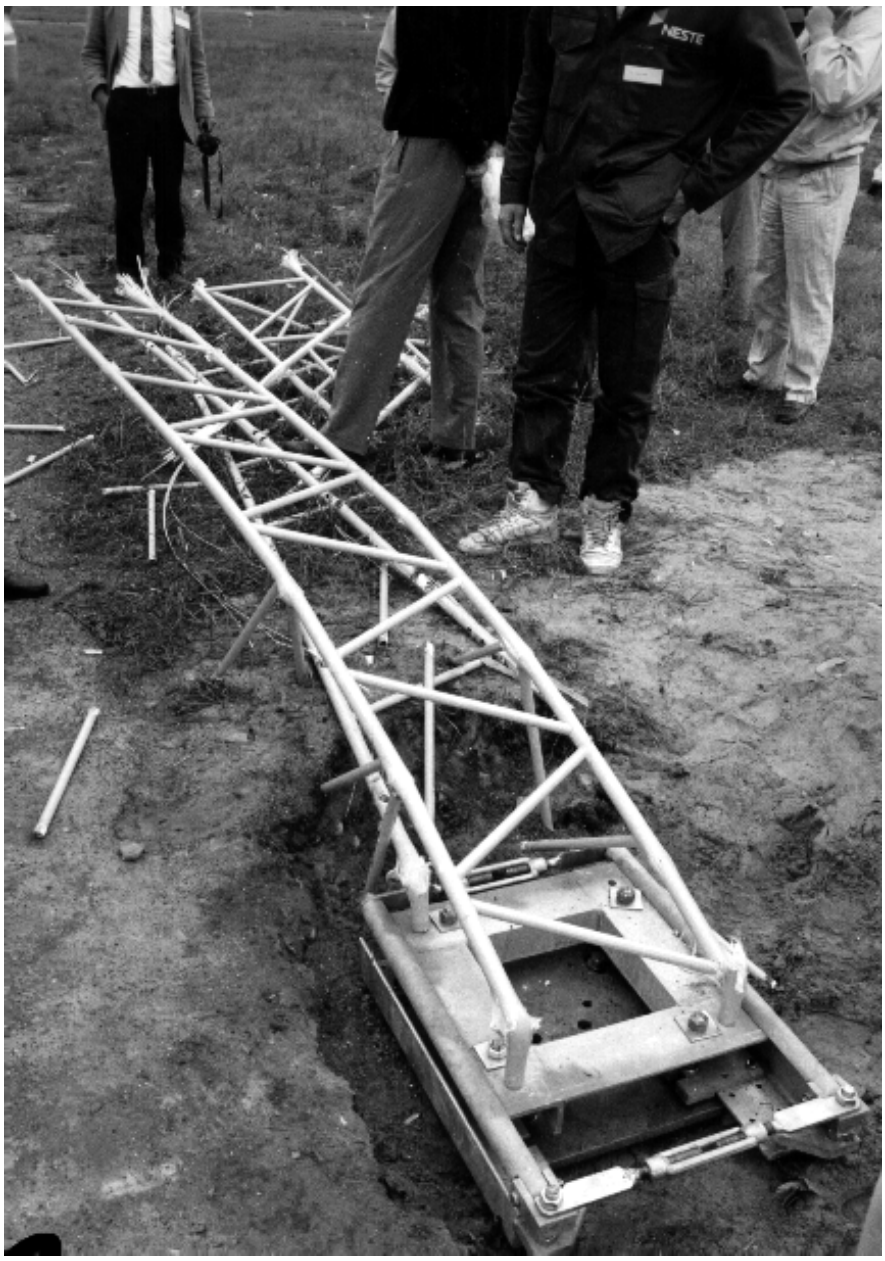

Figure A1.14 The mast was cut through by the impactor. The upper part broke into several parts and the lower section suffered a total collapse when the vertical tubes were bent at the root and most of the diagonals came loose. This is a very good example of the frangible behaviour of the masts.

Figure A1.15 The 400 mm wide mast hit the wing section with 300 mm rib spacing so, that the verticals met the leading edge just on the outer sides of the ribs in the middle. Due to this, all the three leading edge panels were damaged when the diagonals hit the rib section in the middle. Again the damages were limited to the area in front of the front spar.

A1.4 Results from the test 5

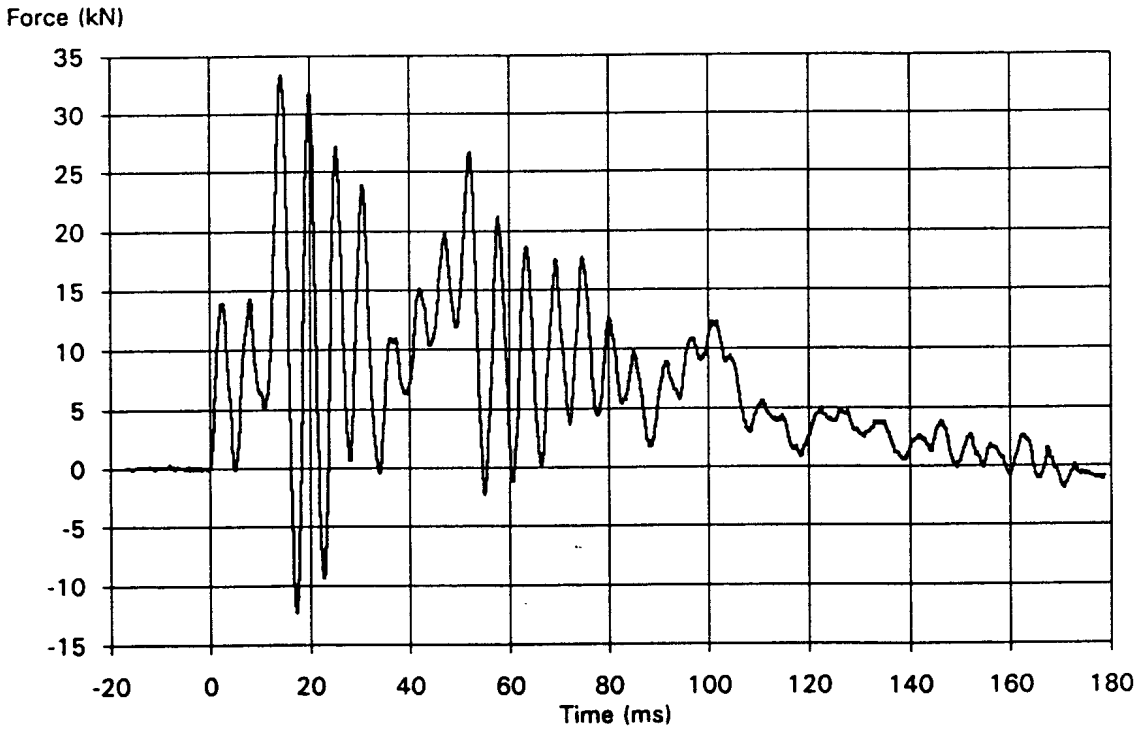

Figure A1.16 Impact forces vs. contact time

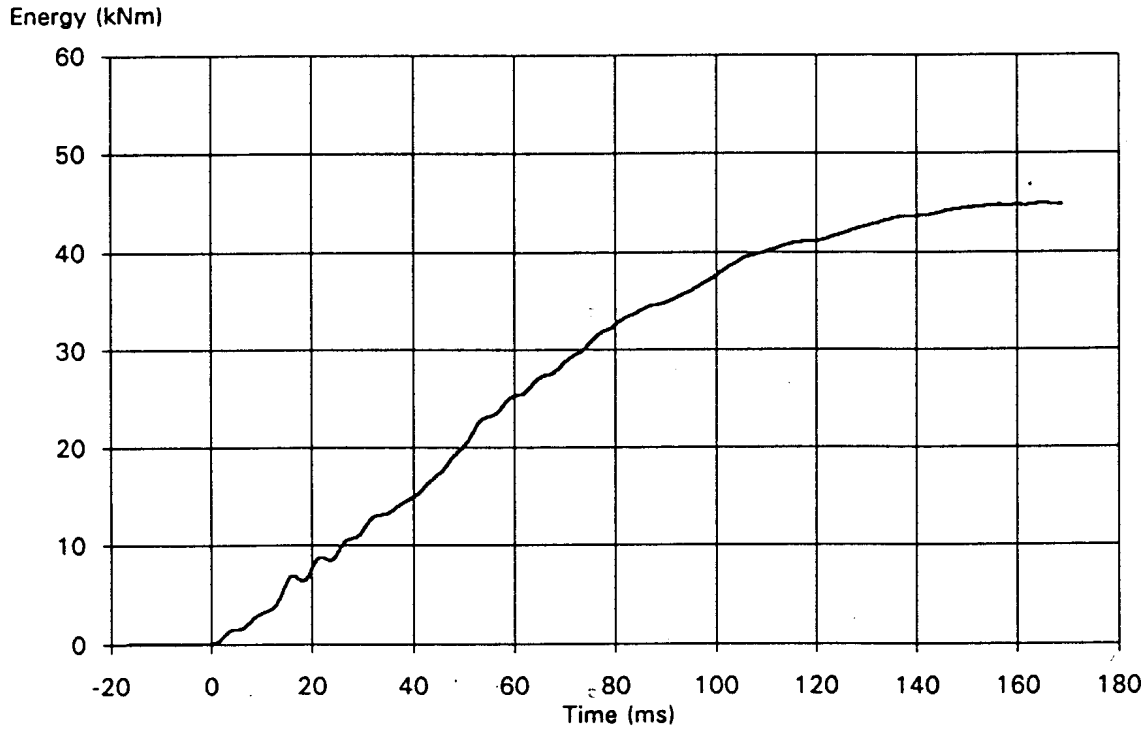

Figure A1.17 Impact energy vs. contact time

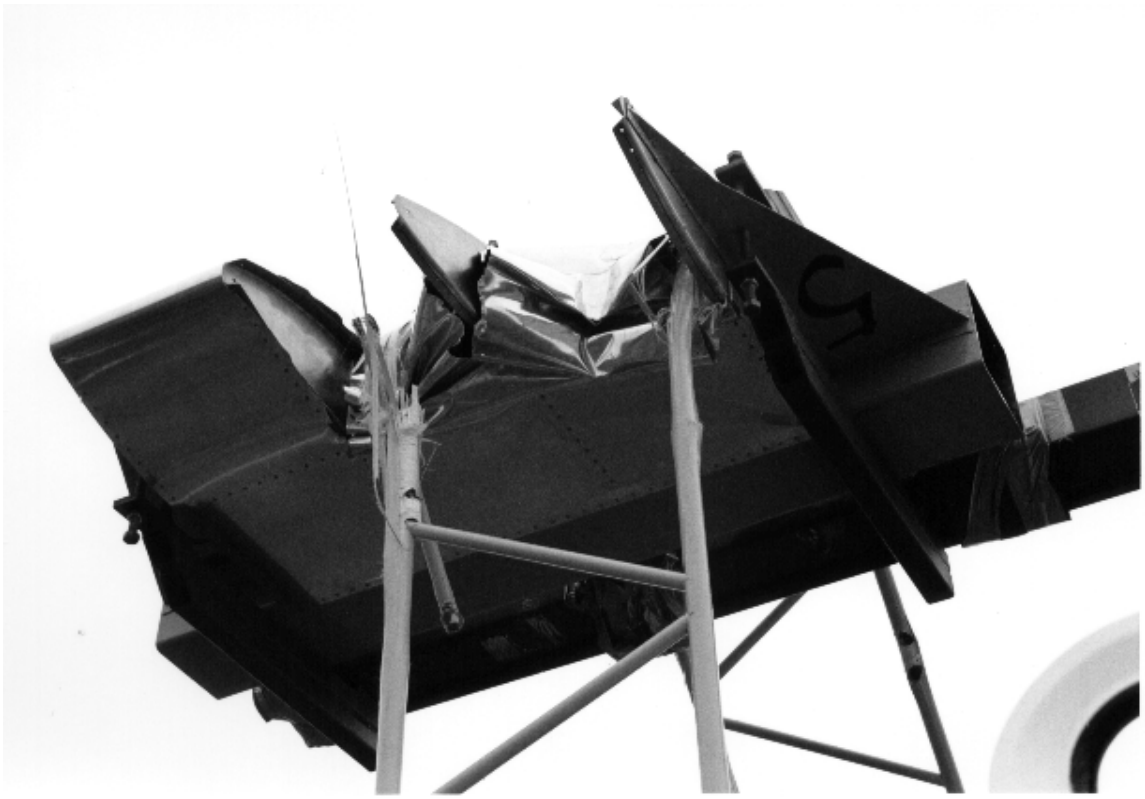

Figure A1. 18 Mast 5 was the first one with cables. The mast showed a tendency to wrap around because neither of the rear verticals was cut by the impactor.

Figure A1.19 The cables and the cover tubes were cut by the impactor as can be seen.

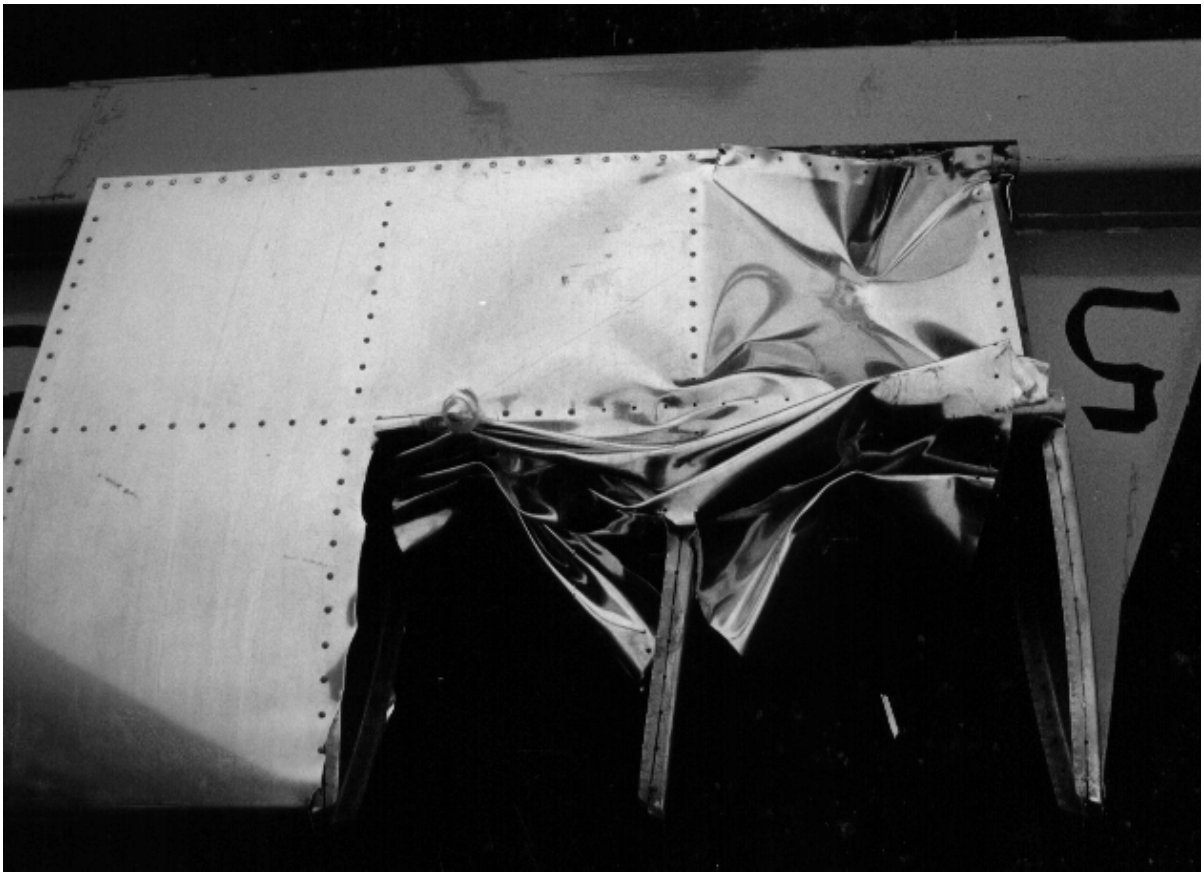

Figure A1.20 Damages were very similar to test 1 except a slight bending of the rib and the deformation in the upper right corner. The latter was caused by a single diagonal that was still attached to the vertical tube when it bent over the wing.

A1.5 Results from the test 6

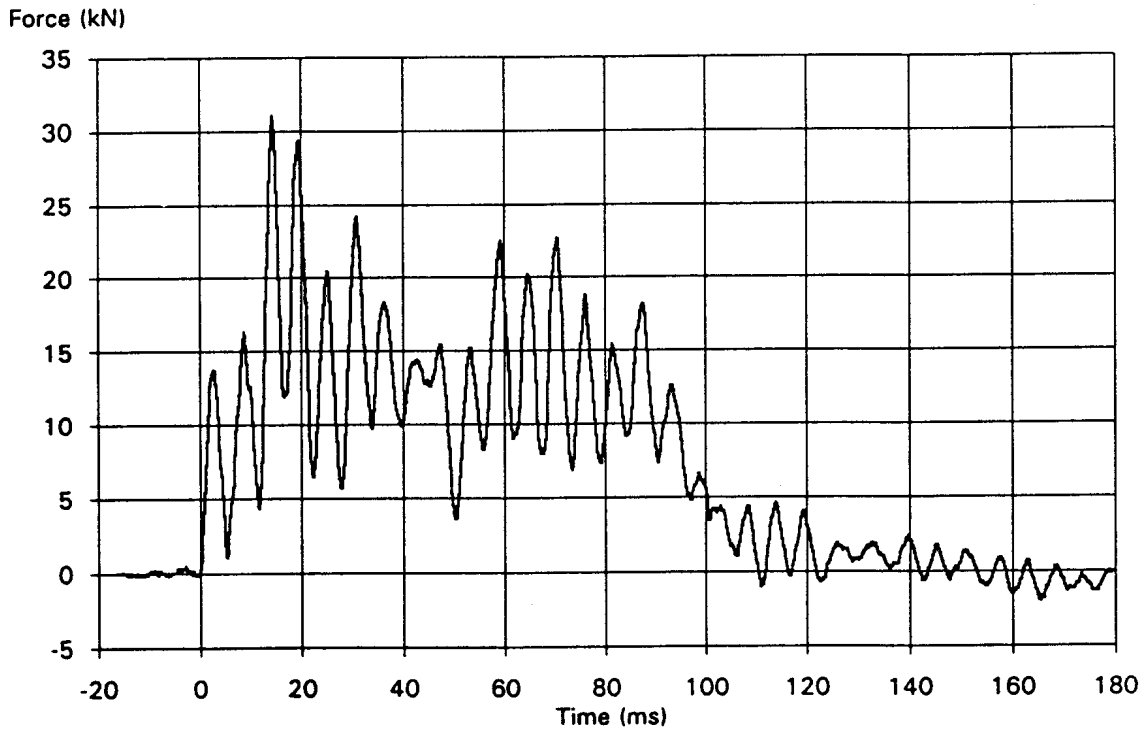

Figure A1.21 Impact forces vs. contact time.

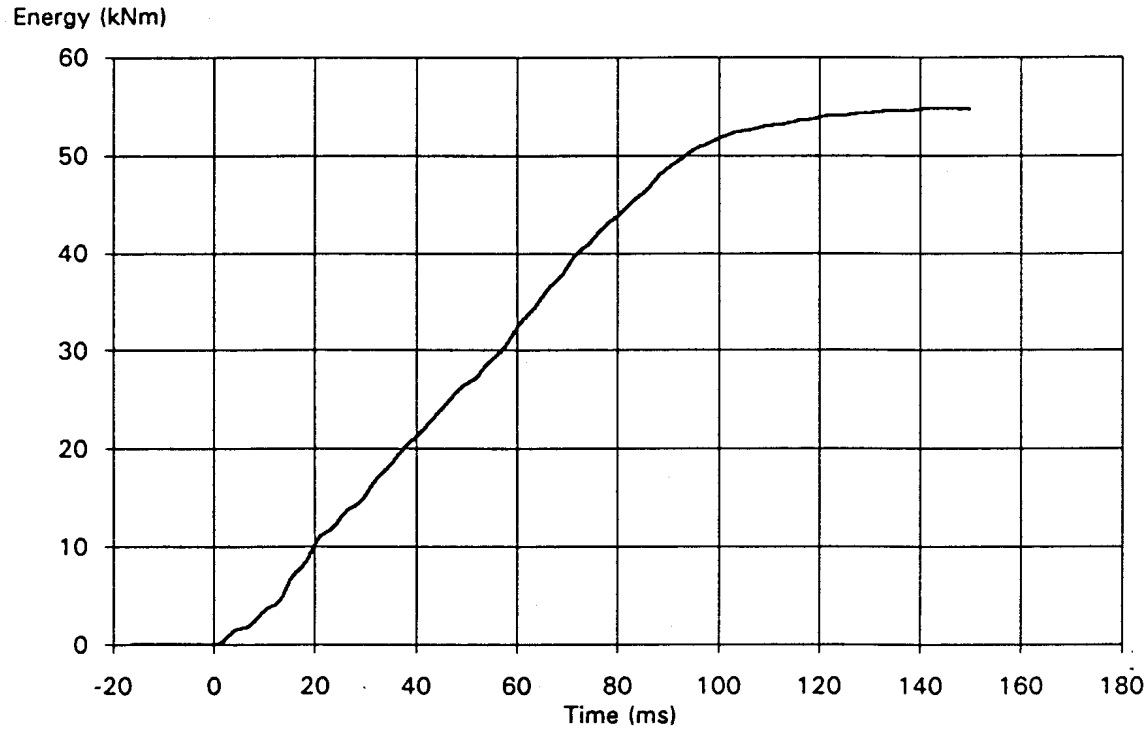

Figure A1.22 Impact energy vs. contact time.

Figure A1.23 Side view of the damaged wing. Damages are very similar to those of tests 1 and 5. The behaviour of the mast was almost identical to the test 5 (not shown).

Figure A1.24 As seen already from the previous picture this a very typical example of the wing section of these tests: two crushed leading edge sections, the next rib section in perfect condition and the front spar intact. It is obvious that an aircraft with this kind of damage would still be able to fly. The fact that this wing section suffered the highest impact energy, could not be detected in the post-impact inspection.

A1.6 Results from the test 7

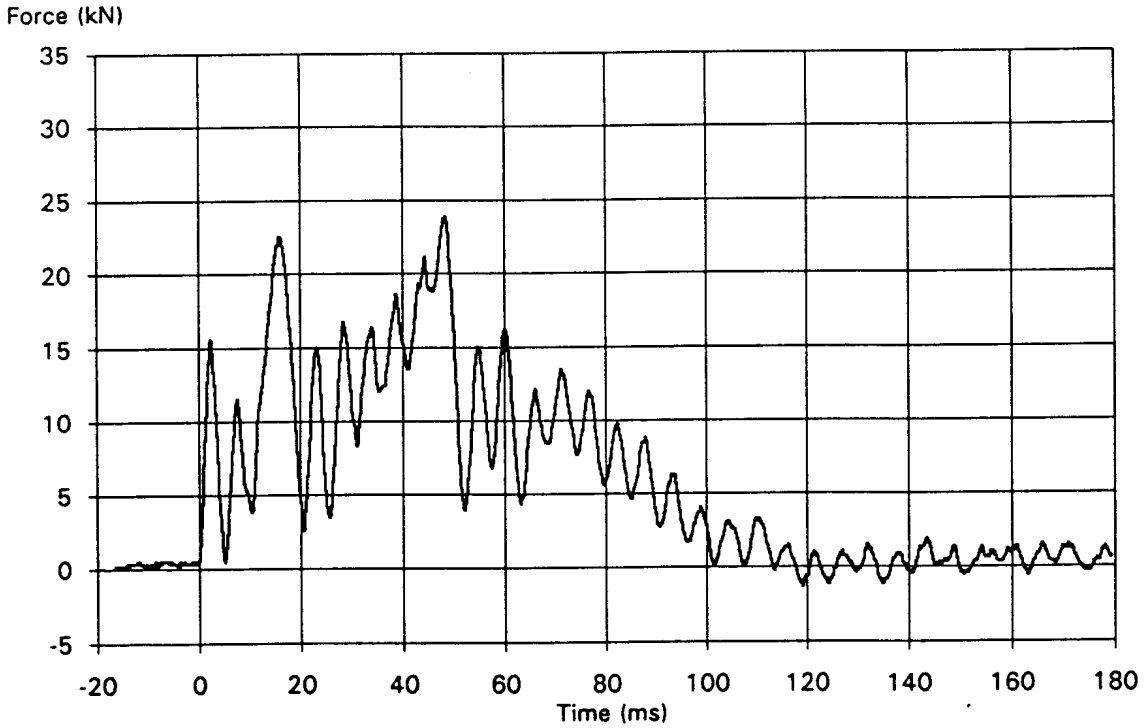

Figure A1.25 Impact forces vs. contact time.

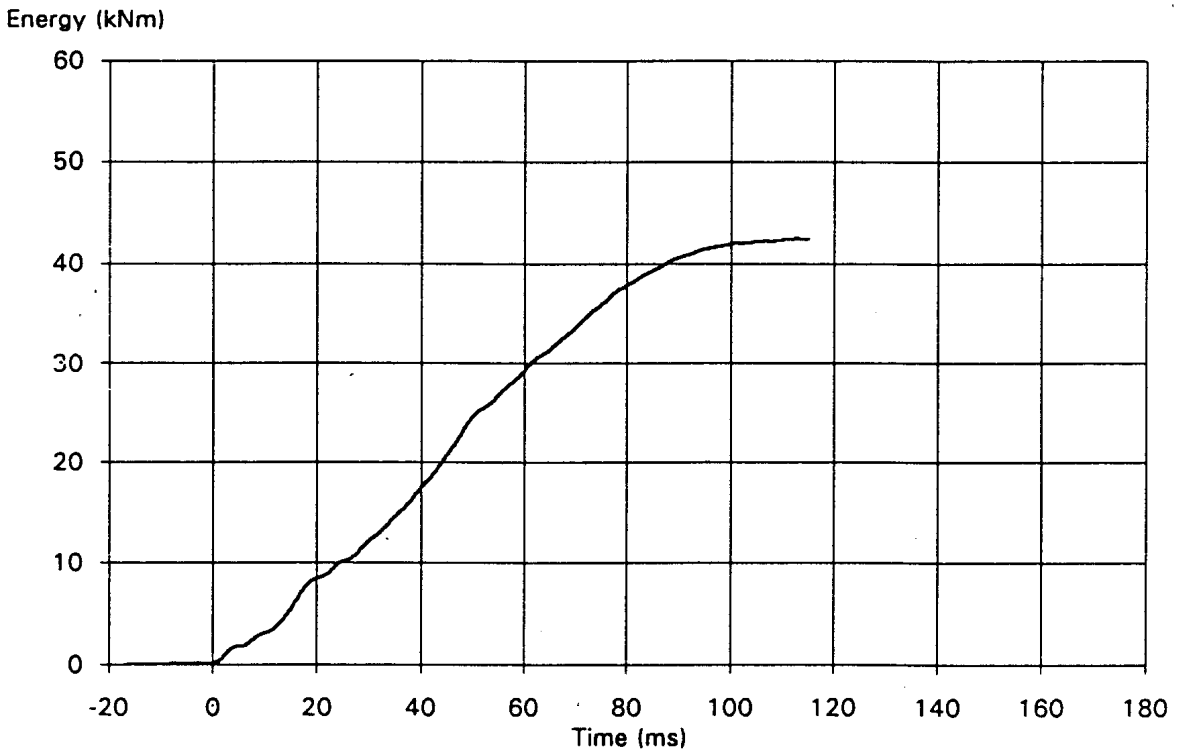

Figure A1.26 Impact energy vs. contact time.

Figure A1.27 In test 7 the mast structure acted like in tests 5 and 6 but the cables and the cover tube failed to cut. In this test they were located at the side of the impact. From the high speed camera recording it can be seen that this is also the side of compressive loading, which is a possible reason to this cable behaviour. It can be seen that again it was the "rear" plane of the lattice structure that bent around the wing section.

Figure A1.28 The lower section of the broken mast was left somewhat shorter in this test. The mast top weight is again visible in the upper right corner.